

High-density linkage maps and chromosome level genome assemblies unveil direction and frequency of extensive structural rearrangements in wood white butterflies (*Leptidea* spp.)

Höök, L.¹*, Näsvall, K.¹*, Vila, R.², Wiklund, C.³, and Backström, N.¹

1. Evolutionary Biology Program, Department of Ecology and Genetics, Uppsala University. Norbyvägen 18D, 752 36 Uppsala, Sweden
2. Butterfly Diversity and Evolution Lab, Institut de Biología Evolutiva (CSIC-UPF), Barcelona, Spain
3. Department of Zoology: Division of Ecology, Stockholm University, Stockholm, Sweden

*Correspondence:

Lars Höök: lars.hook[at]ebc.uu.se

Karin Näsvall: karin.nasvall[at]ebc.uu.se

Evolutionary Biology Program, Department of Ecology and Genetics, Uppsala University.
Norbyvägen 18D, 752 36 Uppsala, Sweden

* Equal author contribution

Keywords: Linkage map, Genome rearrangements, Karyotype evolution, Lepidoptera,

Chromosome fissions/fusions

Running title: Chromosome rearrangements in *Leptidea* butterflies

2 Abstract

3 Karyotypes are generally conserved between closely related species and large chromosome
4 rearrangements typically have negative fitness consequences in heterozygotes, potentially
5 driving speciation. In the order Lepidoptera, most investigated species have the ancestral
6 karyotype and gene synteny is often conserved across deep divergence, although examples
7 of extensive genome reshuffling have recently been demonstrated. The genus *Leptidea* has
8 an unusual level of chromosome variation and rearranged sex chromosomes, but the extent
9 of restructuring across the rest of the genome is so far unknown. To explore the genomes of
10 the wood white (*Leptidea*) species complex, we generated eight genome assemblies using a
11 combination of 10X linked reads and HiC data, and improved them using linkage maps for
12 two populations of the common wood white (*L. sinapis*) with distinct karyotypes. Synteny
13 analysis revealed an extensive amount of rearrangements, both compared to the ancestral
14 karyotype and between the *Leptidea* species, where only one of the three Z chromosomes
15 was conserved across all comparisons. Most restructuring was explained by fissions and
16 fusions, while translocations appear relatively rare. We further detected several examples of
17 segregating rearrangement polymorphisms supporting a highly dynamic genome evolution in
18 this clade. Fusion breakpoints were enriched for LINEs and LTR elements, which suggests
19 that ectopic recombination might be an important driver in the formation of new
20 chromosomes. Our results show that chromosome count alone may conceal the extent of
21 genome restructuring and we propose that the amount of genome evolution in Lepidoptera
22 might still be underestimated due to lack of taxonomic sampling.

23 Introduction

24 The karyomorph is the highest order of organization of the genetic material and
25 understanding the mechanistic underpinnings and micro- and macro-evolutionary effects of
26 changes in chromosome numbers are long-standing goals in evolutionary biology (Mayrose

27 & Lysak, 2021). Chromosome rearrangements have for example been suggested to be
28 important drivers of speciation as a consequence of meiotic segregation problems and
29 suppressed recombination in chromosomal heterozygotes (Faria & Navarro, 2010;
30 Rieseberg, 2001). The number and structure of chromosomes are generally conserved
31 within species and between closely related taxa, while substantial karyotypic changes can
32 occur over longer evolutionary distances (Román-Palacios et al., 2021; Ruckman et al.,
33 2020). In contrast, there are some examples of considerable chromosome rearrangement
34 rate differences between closely related species, but the underlying reasons for why
35 karyotypic change have occurred comparatively rapidly in some lineages are largely
36 unexplored (de Vos et al., 2020; Ruckman et al., 2020; Sylvester et al., 2020). Chromosomal
37 rearrangements, in particular fission and fusion events, are likely often underdominant
38 and/or deleterious and the probability of their fixation in a population should therefore be
39 higher in organisms with lower effective population size (N_e) (Pennell et al., 2015), or with
40 strong meiotic drive (Blackmon et al., 2019). Additionally, the consequences of fissions and
41 fusions seem to depend on the types of chromosomes a species harbor. In species with
42 holokinetic chromosomes (holocentric), the spindle apparatus can bind to multiple positions
43 along the chromosomes, while the attachment is restricted to the specific centromere region
44 in monocentric species (Melters et al., 2012). As a consequence, chromosome fissions and
45 fusions do not necessarily lead to meiotic segregation problems in holocentric species
46 (Faulkner, 1972; Lukhtanov et al., 2018). This has been hypothesized to lead to a higher rate
47 of chromosome number evolution in holocentric compared to monocentric species. However,
48 the evidence for such a rate difference have been mixed and a recent, large-scale meta-
49 analyses across insects suggests that chromosome evolution is not significantly faster in
50 holocentric species (Ruckman et al., 2020), and the explanation for rate differences between
51 species might rather be lineage specific life-history traits or demographics (Kawakami et al.,
52 2009; Larson et al., 1984; Petitpierre, 1987).

53

54 The order Lepidoptera, moths and butterflies, constitutes one of the most species rich and
55 widespread animal groups and has for long been a popular study system in ecology and
56 evolution, in large part due to the high diversity and the eye-catching colour pattern
57 variations that have attracted both amateur naturalists and academic scholars for centuries
58 (Boggs et al., 2003). Lepidoptera also share several key genetic features, like holocentric
59 chromosomes (Suomalainen, 1953), and female heterogamety and achiasmy (Traut et al.,
60 2007; Turner & Sheppard, 1975), which present interesting aspects regarding chromosomal
61 rearrangements and their evolutionary consequences. The karyotype structure has generally
62 been found to be conserved across lepidopteran genera, with most investigated taxa having
63 the inferred ancestral haploid chromosome number of $n = 31$ (de Vos et al., 2020; Robinson,
64 1971). However, the genera *Agrodiaetus* ($n = 10 - 134$, Kandul et al., 2007) and *Godyris* ($n =$
65 13 - 120, Brown et al., 2004), for example, have been shown to have an elevated rate of
66 karyotype evolution compared to other insects (Ruckman et al., 2020). On a more detailed
67 level, genomic analyses have also unveiled a high level of conserved gene synteny between
68 divergent lepidopteran lineages (Ahola et al., 2014; Davey et al., 2016; Pringle et al., 2007).
69 Extensive, genome-wide chromosomal restructuring has so far only been detected in *Pieris*
70 *napi* / *P. rapae* (Hill et al., 2019). However, since the analyses have been limited to a
71 comparatively small set of taxonomic lineages where highly contiguous genome assemblies
72 and / or linkage maps are available, the levels of both karyotype variation and intra-
73 chromosomal rearrangements in Lepidoptera are likely underestimated (de Vos et al., 2020).

74

75 An attractive model system for studying karyotype evolution is the Eurasian wood white
76 butterflies in the genus *Leptidea* (family Pieridae). The three species, common wood white
77 (*Leptidea sinapis*), Réal's wood white (*Leptidea reali*) and the cryptic wood white (*Leptidea*
78 *juvernica*), form a species complex of morphologically nearly indistinguishable species that
79 show remarkable inter- and intraspecific variation in chromosome numbers (Dincă et al.,
80 2011; Lukhtanov et al., 2011). Cytogenetic analyses have shown that *L. reali* has rather few
81 chromosomes and less intraspecific variation ($n = 25 - 28$), while *L. juvernica* has a

82 considerably more fragmented and variable karyotype ($n = 38 - 46$) (Dincă et al., 2011;
83 Šíchová et al., 2015). The most striking chromosome number variation has been found in *L.*
84 *sinapis*, which has one of the most extreme non-polyplid, intraspecific karyotype clines of
85 all eukaryotes, ranging from $n \approx 53 - 55$ in southern Europe and gradually decreasing to $n \approx$
86 28 – 29 in northern Europe and $n \approx 28 - 31$ in central Asia (Lukhtanov et al., 2011, 2018). In
87 addition, the common ancestor of the species complex has undergone translocations of
88 autosomal genes to the sex chromosome(s) and extension of the ancestral Z chromosome
89 that has resulted in a set of neo sex chromosomes (Šíchová et al., 2015; Yoshida et al.,
90 2020). *Leptidea* butterflies have also experienced a relatively recent burst of transposable
91 element activity (Talla et al., 2017), elements that could act as important drivers of
92 chromosome rearrangements (Belyayev, 2014), but whether this has been important for
93 karyotype evolution specifically in this genus remains to be explored. Altogether, these
94 findings motivate detailed characterization of the rate and direction of the chromosome
95 rearrangements and assessment of potential drivers of the rapid karyotype changes in this
96 lineage.

97

98 In order to dissect the chromosome structure in detail and quantify rates and directions of
99 chromosome rearrangements, we sequenced and assembled the genome of a male and
100 female individual of *L. juvernica*, *L. reali* and the Swedish and Catalan populations of *L.*
101 *sinapis* using a combination of 10X linked reads and HiC-scaffolding. In addition, we
102 generated genetic maps for the two *L. sinapis* populations and used the linkage information
103 to super-scaffold and correct the physical genome assemblies. The assembled
104 chromosomes were compared between wood white species and with the inferred ancestral
105 lepidopteran karyotype to characterize rates and patterns of fissions, fusions and intra-
106 chromosomal rearrangements across the species complex. Furthermore, we quantified
107 enrichment of different types of genetic elements in fission and fusion breakpoints to assess
108 if specific genomic features have been associated with chromosome rearrangements.

109 Results

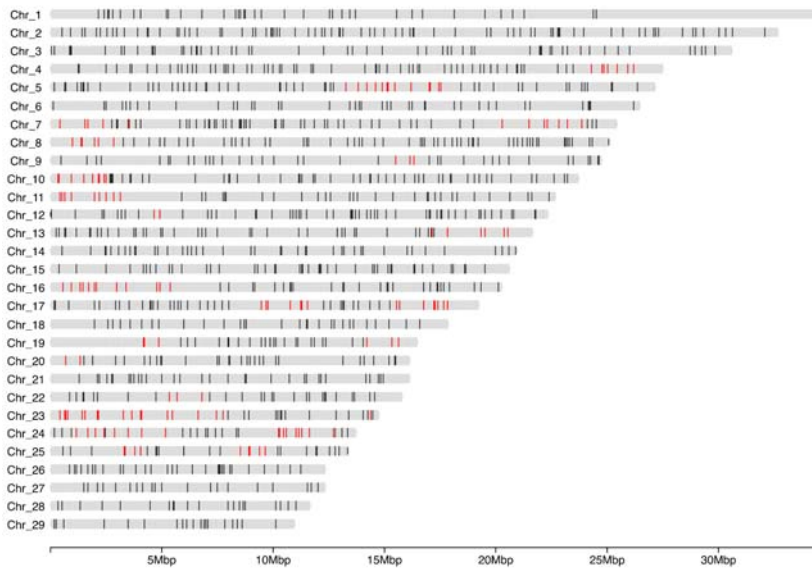
110 The genome assemblies had extensive contiguity, high BUSCO scores (Supplementary
111 table 1), few gaps and the majority of sequence contained in chromosome-sized scaffolds
112 (Table 1, Supplementary figures 1 and 2). The implementation of linkage map information for
113 the Swedish and Catalan *L. sinapis* (Figure 1) allowed for correction of these particular
114 genome assemblies. Overall, we found a high level of collinearity between physical maps
115 and linkage maps, but several large inversions were corrected (Supplementary figure 3). The
116 Catalan *L. sinapis* male assembly was also compared to the DToL assembly of a *L. sinapis*
117 male from Asturias at the north-western Iberian Peninsula (Lohse et al., 2022). Apart from
118 differences which likely represent genuine rearrangements (see ‘Chromosome
119 rearrangements’), there was a high level of collinearity between these two assemblies
120 (Supplementary figure 4).

Table 1. Estimated summary statistics for the 8 different *Leptidea* genome assemblies.

Statistic	<i>L. juvernica</i> female	<i>L. juvernica</i> male	<i>L. reali</i> female	<i>L. reali</i> male	<i>L. sinapis</i> Swedish female	<i>L. sinapis</i> Swedish male	<i>L. sinapis</i> Catalan female	<i>L. sinapis</i> Catalan male
Assembly size (Mb)	675	660	670	642	685	664	672	655
Sequence N's (%)	3.4%	4.1%	3.7%	2.4%	5.4%	5.6%	3.3%	3.8%
GC (%)	35.6%	35.5%	35.4%	35.3%	35.4%	35.3%	35.4%	35.4%
Predicted genes (N)	-	16 149	-	15 689	-	15 915	-	16 478
BUSCO genes (%)	93.7%	95.0%	93.4%	93.4%	93.9%	93.8%	94.6%	94.5%
Pseudo- chromosomes (N)	43	42	26	26	28	29	52	52
Sequence in Pseudo- chromosomes (%)	83.3%	90.7%	88.0%	88.4%	89.2%	90.2%	89.2%	90.4%
Read mapping (%)	98.2%	98.6%	98.3%	98.0%	98.1%	98.6%	98.2%	98.2%
Repeat content (%)	54.6%	52.0%	52.0%	54.1%	52.0%	51.3%	53.6%	53.2%
Scaffolds (N)	20 731	16 073	16 210	15 448	17 536	16 022	17 757	16 290
Scaffold N50 (Mb)	15.087	15.702	22.890	21.966	24.480	21.838	11.055	11.044

Contigs (N)	36 909	30 088	29 081	28 137	31 643	29 387	31 619	31 643
Contig N50 (kb)	65.133	79.484	81.855	82.283	72.761	73.965	78.960	79.404

a)



b)

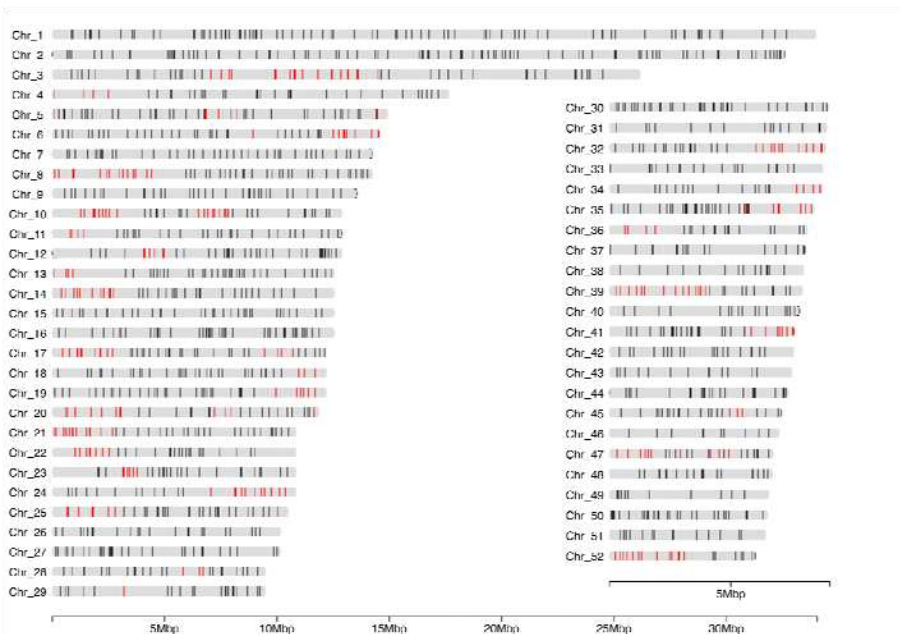


*Figure 1. Linkage maps based on pedigrees for a) the Swedish, and b) the Catalan populations of *L. sinapis*. Vertical bars on each chromosome represent the position of linkage informative markers ordered according to the physical map (genome assembly). The x-axis represents the physical*

position of each marker in megabases (Mb). Red colour represents markers where the marker order in the linkage map was found to deviate from the order in the preliminary physical assembly.

121

122 *Chromosome rearrangements*

123 In order to characterize how chromosomes in the *Leptidea* clade correspond to the
124 presumably nearly ancestral lepidopteran karyotypes of *B. mori* and *M. cinxia*, gene orders
125 were compared between the different lineages (Figure 2). The synteny analysis revealed a
126 considerable amount of large rearrangements where each *Leptidea* chromosome showed
127 homology to 3 - 5 (median) *B. mori* chromosomes (Figure 2, Supplementary figure 5,
128 Supplementary table 2). Not only have all chromosomes in *Leptidea* been restructured
129 compared to the ancestral lepidopteran karyotype, but the frequency of rearrangements
130 between *Leptidea* species was also high. Only one of the sex chromosomes (Z2) showed
131 conserved synteny across all *Leptidea* species (Figure 2). When compared to *B. mori*, the
132 *Leptidea* genomes contained 372 - 410 distinct synteny blocks. The synteny blocks ranged
133 between 0.94 - 1.00 Mb, corresponding to 12.5 - 14.5 blocks per chromosome, and
134 contained 24 - 25 genes (medians given; Supplementary table 2).

135

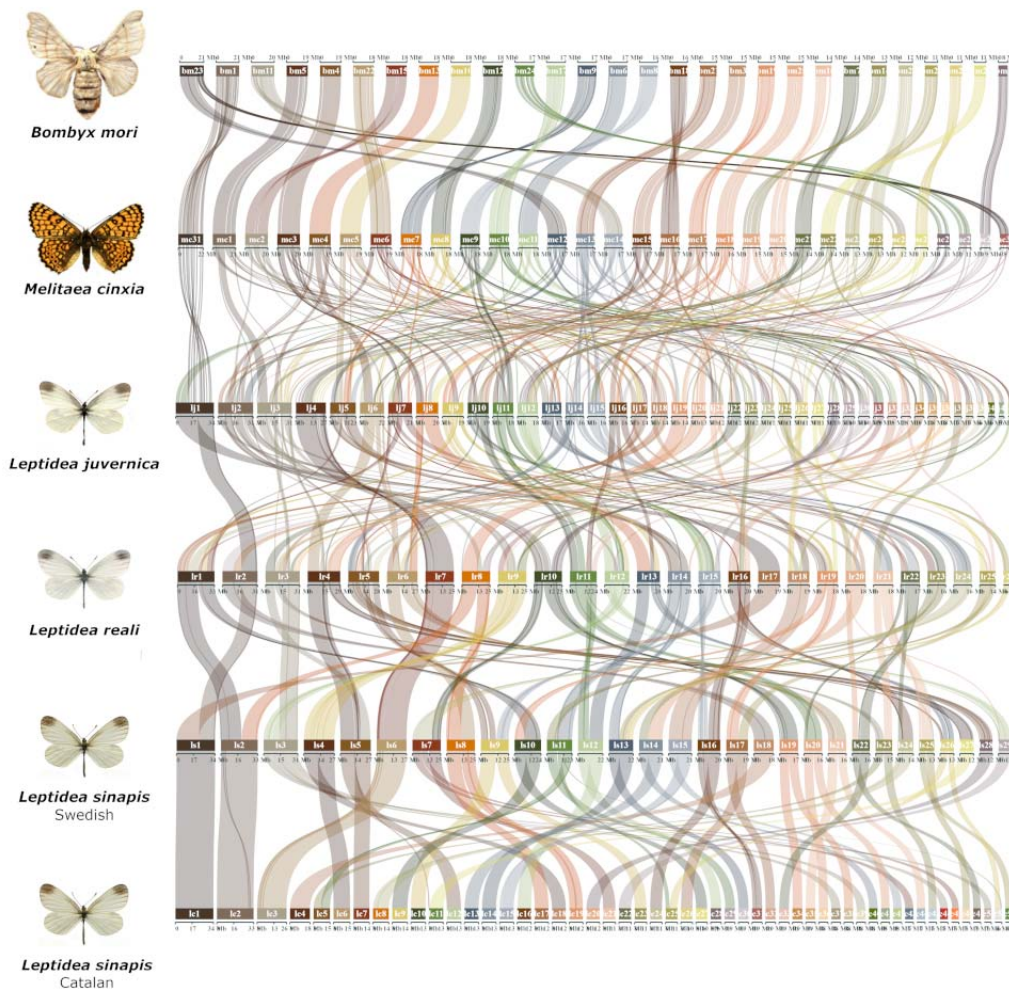


Figure 2. Comparison of synteny between the *Leptidea* species and the two references *B. mori* and *M. cinxia*. The karyotype of the latter species is assumed to represent the ancestral lepidopteran karyotype (Ahola et al., 2014). Chromosomes are ordered by size in each species. Pair-wise comparisons between *B. mori* and each respective *Leptidea* lineage are available in Supplementary Figure 5.

136 Since equivalent large-scale genome restructuring was recently shown in another pierid
137 butterfly, *P. napi* (Hill et al., 2019), we also compared synteny between *P. napi* and the
138 different *Leptidea* species. Apart from one syntenic chromosome pair (*P. napi* chromosome
139 18 and Catalan *L. sinapis* chromosome 31), all chromosome pairs in the comparisons
140 contained a mix of synteny blocks from at least two different chromosomes, indicating that

141 the absolute majority of rearrangements in *P. napi* and *Leptidea* have occurred
142 independently in the two different lineages (Supplementary figure 6).

143

144 After discovering the considerable genomic reorganizations in *Leptidea*, we aimed at
145 characterizing the different rearrangements in more detail. A phylogenetic approach was
146 implemented to infer the most parsimonious scenario for intra-specific chromosome
147 rearrangements. In *L. sinapis*, the data indicate that 9 fusions have occurred in the Swedish
148 population (Supplementary figure 7) and 8 fissions (Supplementary figure 8) and two fusions
149 (Supplementary figure 7) in the Catalan population. In addition, there were 8 cases of shared
150 breakpoints between the Catalan *L. sinapis* and *L. juvernica* (Supplementary figure 8), which
151 explain the majority of the remaining differences in chromosome numbers between Catalan
152 and Swedish *L. sinapis*. Such shared breakpoints could either represent sorting of ancestral
153 fissions, independent fissions at the same chromosome positions in Catalan *L. sinapis* and
154 *L. juvernica*, or independent, identical fusions in *L. reali* and Swedish *L. sinapis*. If fusions
155 tend to occur randomly, we expected that chromosome pairs that have fused independently
156 in two different lineages could have different orientations. However, in all cases except one,
157 where a small inversion was in close proximity to a breakpoint, the chromosomes were
158 collinear between *L. reali* and Swedish *L. sinapis*, suggesting that the ancestral state has
159 been retained in both species. The two *L. sinapis* populations also shared five ancestral
160 fusions (Supplementary figure 7), but no shared fissions. In addition, four of the fissions
161 identified in the Catalan *L. sinapis* were not present in the individual from Asturias
162 (Supplementary figure 4). In *L. reali* we identified 21 fusions (Supplementary figure 9) and
163 six fissions (Supplementary figure 10) in total. We cannot exclude that some of these events
164 correspond to chromosome translocations rather than fissions and fusions, since all except
165 one of the fissioned chromosomes also have been involved in fusions. Finally, in the
166 comparison between *L. juvernica* on the one hand and *L. sinapis* / *L. reali* on the other, we
167 found 51 chromosome breakpoints shared by *L. sinapis* / *L. reali* (fusion in *L. juvernica* or

168 fission in *L. sinapis* / *L. reali*) and 44 unique breakpoints in *L. juvernica* (fission in *L. juvernica*
169 or fusion in *L. sinapis* / *L. reali*).

170

171 The extreme rate of chromosomal rearrangements observed within the *Leptidea* clade
172 motivated further comparison to the ancestral Lepidopteran karyotype. We therefore tested
173 how often coordinates of the previously identified chromosome breakpoints overlapped with
174 breaks in synteny between *M. cinxia* and *Leptidea*. Synteny breaks were inferred when
175 consecutive alignment blocks switched from one chromosome to another in *M. cinxia*. This
176 analysis showed that 33 of the 37 fusions previously called in *L. sinapis* and *L. reali*
177 overlapped with synteny breakpoints in *M. cinxia* (33 / 37 overlapping fusions is significantly
178 different from a random genomic occurrence of overlaps; randomization test, p-value <
179 1.0×10^{-5} ; Supplementary figure 11), verifying that these constitute novel rearrangements in
180 *Leptidea*. The four exceptions included one fusion in *L. sinapis* and three fusions in *L. reali*.
181 These cases could represent fissions in the ancestral *Leptidea* lineage followed by recurrent
182 fusions in a specific species, or fissions that occurred independently in *L. juvernica* and *M.*
183 *cinxia*. Three of 14 previously characterized fissions in *Leptidea* and four of 8 chromosome
184 breakpoints shared between *L. juvernica* and Catalan *L. sinapis* overlapped synteny breaks
185 in *M. cinxia* and therefore likely rather represent fusions in a *Leptidea* lineage than
186 independent fissions in *M. cinxia* and one of the *Leptidea* species.

187

188 In cases where chromosome rearrangements within *Leptidea* were not supported based on
189 homology information in *M. cinxia*, we analyzed the breakpoint regions for presence of
190 telomeric repeats (TTAGG)n or (CCTAA)n, which should only be present if the rearranged
191 region corresponds to a chromosome fusion. For the inferred fusion shared by both *L.*
192 *sinapis* populations, we found telomeric repeats in both the Swedish and Catalan individuals,
193 indicating that this represents a fusion back to the ancestral state. Conversely, the three
194 fusions in *L. reali* did not contain any telomeric repeats which indicates that several fissions
195 have occurred in the same chromosome region in different *Leptidea* lineages, or that

196 ancestral fission/fusion polymorphisms have sorted differently within the *Leptidea* clade.
197 Regions around one fission in Catalan *L. sinapis* and two fissions in *L. reali* that were not
198 supported by homology information in *M. cinxia* also lacked telomeric repeats in the other
199 *Leptidea* lineages. These three fissions therefore likely occurred within regions that
200 represent chromosome fusions that pre-date the radiation of the *Leptidea* clade. Finally, two
201 of the four shared fission breakpoints between *L. juvernica* and Catalan *L. sinapis*, which
202 were fusion-like compared to *M. cinxia*, did not contain telomeric repeats in the other
203 *Leptidea* samples and therefore likely represent fissions. All inferred fission and fusion
204 events are summarized in Figure 3 and Supplementary table 3. We further polarized the
205 chromosome breakpoints identified between *L. juvernica* and the other *Leptidea* species.
206 Here, 46 of 51 *L. reali* / *L. sinapis* chromosome breakpoints (fusion in *L. juvernica* or fission
207 in *L. reali* / *L. sinapis*) and 16 of 44 breakpoints in *L. juvernica* (fission in *L. juvernica* or
208 fusion in *L. reali* / *L. sinapis*) had overlapping synteny breaks in *M. cinxia*, indicating that the
209 majority (65.3%) represent fusions that have occurred within the *Leptidea* clade. The
210 directions and frequencies of chromosome rearrangements in the different lineages suggest
211 that the common ancestor of the three investigated *Leptidea* species had a haploid
212 chromosome number ($n \sim 51-53$) close to that of present day Catalan *L. sinapis*.

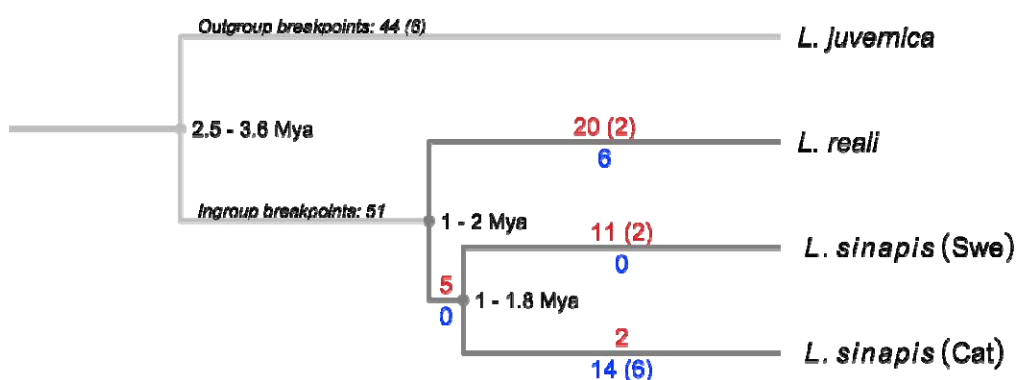


Figure 3. Estimated number of chromosomal rearrangement events in the different *Leptidea* species/populations. Fusions are highlighted in red and fissions in blue. Numbers show total counts

for each branch and shared events are shown in parenthesis. Divergence times are based on Talla et al. (2017).

213 Next, we estimated how much of the observed rearrangements could alternatively be the
214 result of translocations. First, we checked for exchange of homologous regions between
215 chromosomes and species, which could be an indication of reciprocal translocations. For the
216 ingroup species (*L. sinapis* and *L. reali*) we only detected one such case in Catalan *L.*
217 *sinapis* involving chromosomes 25 and 51. Next, we counted how often a chromosome
218 region was flanked by regions from one other chromosome in another species which could
219 indicate a non-reciprocal, internal translocation event. Here, we also only detected one case,
220 in *L. reali* chromosome 20. Finally, since translocations do not necessarily affect
221 chromosome ends, we counted how many ancestral chromosome ends (compared to *B.*
222 *mori*) were still present in *Leptidea* and how many of these were kept as ancestral pairs. This
223 showed that few ancestral chromosome ends are maintained (*L. juvernica*: 10/84, *L. reali*:
224 7/52, Swedish *L. sinapis*: 11/56, Catalan *L. sinapis*: 18/104) and no ends remain paired in
225 any of the species. Taken together, this suggests that translocations are rare and most
226 rearrangements have occurred through fissions and fusions.

227

228 *Intraspecific rearrangements*

229 The high frequency of interspecific chromosome rearrangements between *Leptidea* species
230 spurred an additional set of analysis to assess occurrences and frequencies of fission /
231 fusion polymorphisms segregating within the populations. While the physical assemblies of
232 the male and female *L. reali* and Catalan *L. sinapis*, respectively, were collinear, we found
233 evidence for fission / fusion polymorphisms segregating within both *L. sinapis* and *L.*
234 *juvernica* (Supplementary figure 12). First, the Catalan (C) and Asturian (A) *L. sinapis*
235 individuals, which presumably represent populations with recent shared ancestry, had highly
236 similar karyotypes, but we found one fusion polymorphism (C 5 = A 6 + A 45; A 6 = C 5 + C
237 51; Supplementary figure 4) and a potential translocation involving chromosomes C 6 and C

238 18 + A 10 and A 18, respectively (Supplementary figure 4). Second, within the Swedish *L.*
239 *sinapis*, the comparison of the male and the female assemblies revealed two segregating
240 chromosome fusions ($\text{♀ 3} = \text{♂ 19} + \text{♂ 25}$, and $\text{♀ 6} = \text{♂ 21} + \text{♂$
241 28) (Supplementary figure 12 and 13) and two cases where the male and female were
242 heterozygous for different rearrangement polymorphisms ($\text{♀ 4} = \text{♂ 5} + \text{♂ 27}$; $\text{♂ 5} = \text{♀ 4} + \text{♀}$
243 27, and $\text{♀ 10} = \text{♂ 11} + \text{♂ 26}$; $\text{♂ 11} = \text{♀ 10} + \text{♀ 26}$) (Figure 4, Supplementary figure 12). In the
244 first case ($\text{♀ 4} = \text{♂ 5} + \text{♂ 27}$; $\text{♂ 5} = \text{♀ 4} + \text{♀ 27}$), the fusion point between chromosomes ♀ 4
245 and ♂ 5 appears to be associated with a large inversion (supported by the linkage map data,
246 see below), which connects the fused variants in different orientations. To understand the
247 background of these two complex rearrangement polymorphisms, we analyzed the
248 homologous regions in the other *Leptidea* populations / species. For the first case, we found
249 that *L. reali* shared the fusion variant observed in the *L. sinapis* female (i.e. $\text{♀ 4} = \text{♂ 5} + \text{♂}$
250 27; likely the ancestral state) while the Catalan and Asturian *L. sinapis* shared the variant
251 observed in the Swedish *L. sinapis* male ($\text{♂ 5} = \text{♀ 4} + \text{♀ 27}$), with an additional fission within
252 the inverted region. In *L. juvernica*, the genomic regions involved in rearrangement
253 polymorphisms in the Swedish *L. sinapis* were separate chromosomes. In the second case
254 ($\text{♀ 10} = \text{♂ 11} + \text{♂ 26}$; $\text{♂ 11} = \text{♀ 10} + \text{♀ 26}$), both *L. reali* (chromosome 14) and *L. juvernica*
255 (5) shared the variant observed in the Swedish *L. sinapis* male ($\text{♂ 11} = \text{♀ 10} + \text{♀ 26}$) with
256 several additional rearrangements around the fusion point. The constitution in Catalan and
257 Asturian *L. sinapis* was also most similar to the variant observed in the Swedish *L. sinapis*
258 male but with additional smaller rearrangements connected to it. Hence, the variant
259 observed in the Swedish *L. sinapis* female ($\text{♀ 10} = \text{♂ 11} + \text{♂ 26}$) appears to be specific to
260 this population (Figure 4).

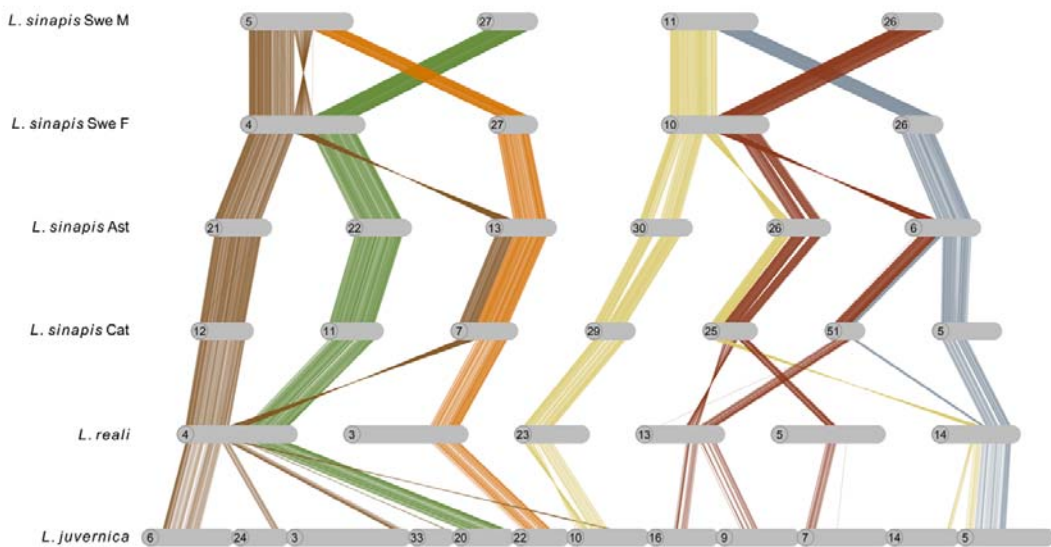


*Figure 4. Fusion polymorphisms in Swedish *L. sinapis* and respective homologous regions in the other *Leptidea* species and populations. Lines show individual alignments (> 90% similarity) and colours represent homologous regions. Chromosomes have been rotated to enhance visualization. Note that chromosomes 26 and 27 are not homologous to the chromosome with the same number in the opposite sex in Swedish *L. sinapis*. Ast: Asturias population, Cat: Catalan population.*

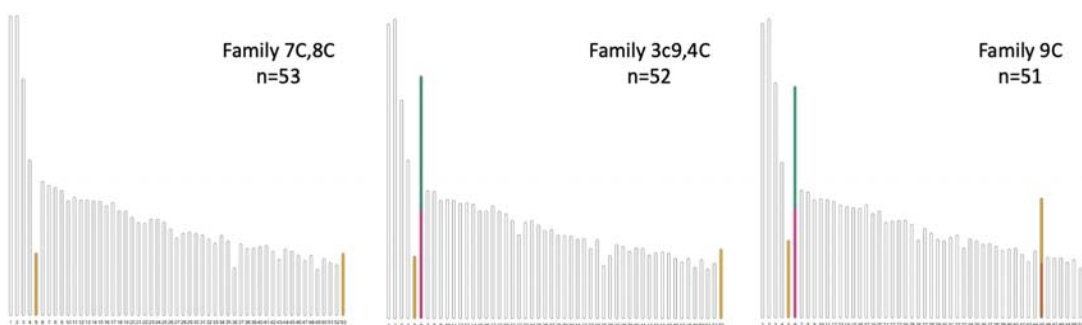
261 Finally, when comparing the male and the female *L. juvernica* assemblies, we also detected
262 three segregating fusions ($\text{♀ } 5 = \text{♂ } 24 + \text{♂ } 25$; $\text{♂ } 17 = \text{♀ } 28 + \text{♀ } 38$; $\text{♂ } 41 = \text{♀ } 42 + \text{♀ } 43$;
263 supplementary figure 14) and one rearrangement polymorphisms; $\text{♀ } 20 = \text{♂ } 27 + \text{♂ } 37$; $\text{♂ } 27$
264 $= \text{♀ } 20 + \text{♀ } 40$; Supplementary figure 15).

265

266 The intraspecific chromosome rearrangement polymorphisms observed with the HiC-maps
267 obviously only reflects the variation between two individuals in each population. To provide
268 information from more individuals in each population and assess the frequency of
269 segregating rearrangement polymorphisms in more detail, we used the pedigrees to
270 construct single family based linkage maps in the populations with the largest difference in
271 chromosome count - the Swedish and the Catalan *L. sinapis*. This independent analysis
272 verified the observations from the HiC-maps, and revealed additional segregating

273 chromosome rearrangement polymorphisms. For the Swedish population, we could
274 construct linkage maps for four independent families and they all had different karyotypes
275 when compared to the Swedish *L. sinapis* male genome assembly. Family T4 had one of the
276 chromosome fusions (δ 21 + δ 28) and family T3 two additional fusions (δ 27 + δ 5, δ 11 +
277 δ 26) that were observed when comparing the male and female genome assemblies. In
278 family T5 we observed the same fusions as in family T3 but with additional fissions involving
279 δ 7 and δ 11. Some of the previously identified fusions and the fission of chromosome δ 7
280 were also observed in family T2. Hence, the linkage analysis in independent families
281 confirmed the fission / fusion polymorphisms identified in the comparison between genome
282 assemblies and revealed an additional fission of δ 7 in two families. For the Catalan families
283 we could construct five independent maps. Here we observed three different karyotypes, all
284 differing from the genome assembly of the Catalan *L. sinapis* male. A fission of chromosome
285 δ 5 was present in all families, similar to the observation in the Asturian *L. sinapis*. In three
286 families, 3c9, 4C and 9C, we found a fusion of δ 6 + δ 18 and in addition to δ 6 + δ 18
287 there was also one part of δ 5 fused to δ 45 in family C9. In summary, the genetic maps for
288 independent families provide evidence for several chromosome rearrangement
289 polymorphisms that are currently segregating in the different populations (Figure 5).

a)



b)

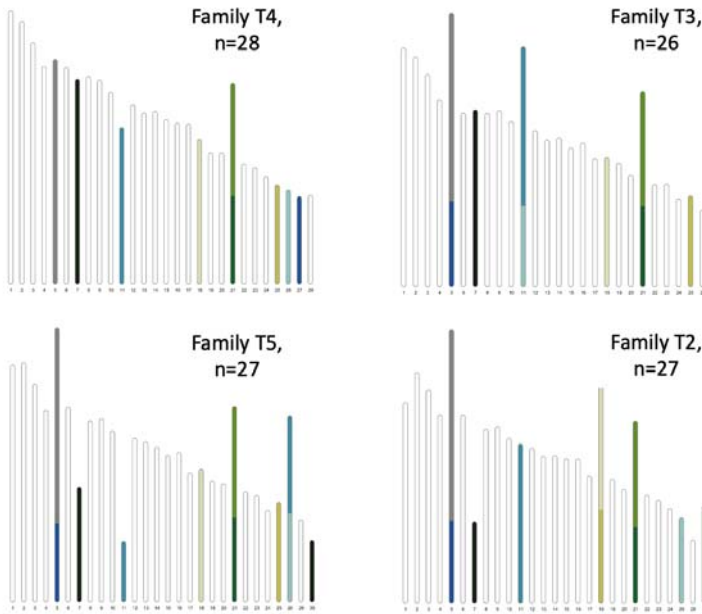


Figure 5. Linkage groups for a) Swedish families and b) Catalan *L. sinapis* families. Colours represent specific chromosomes in the male genome assembly for the Swedish ($n = 26 - 28$) and Catalan ($n = 51 - 53$) *L. sinapis* population, respectively.

290 *Structural variation in the sex chromosomes*

291 The synteny of the Z chromosomes agreed with previous results (Yoshido et al., 2020) and
292 in addition we detected previously unknown gene movement from *B. mori* autosomes 19, 26
293 and 28 to the sex chromosomes in *Leptidea* (Supplementary figure 16). In *L. sinapis*, we
294 identified the three previously described Z chromosomes and a female specific ~ 4.4 Mb
295 long scaffold, which likely represents (at least part of) the W chromosome. No equivalent W
296 scaffold was observed in the Catalan *L. sinapis* female assembly. We noticed however that
297 Z chromosome 3 in the two female *L. sinapis* assemblies and Z chromosome 1 in *L. reali*
298 were several Mb longer than their male homologs and that they aligned less well compared
299 to other chromosomes, indicating that these scaffolds likely are chimeras between the Z and
300 W chromosome parts. In *L. reali*, we also discovered a previously unknown translocation
301 event between what has previously been identified as Z chromosome 1 and Z chromosome
302 3 (Yoshido et al., 2020; Supplementary figure 16). One of these lineage specific Z
303 chromosomes contains a major part of the ancestral Z which has fused with Z chromosome

304 3. The other contains the remaining ancestral and neo parts of Z chromosome 1. This was
305 observed in both the male and the female.

306

307 *Sequence analysis of the fissioned and fused chromosome regions*

308 In agreement with previous data (Talla et al., 2017), we found that the TE content was >
309 50% in all *Leptidea* assemblies (Table 1) and the majority of the TEs were long interspersed
310 nuclear elements (LINEs; Supplementary figure 17). Since TEs may facilitate structural
311 rearrangements (Miller & Capy, 2004), we assessed potential associations between specific
312 sequence motifs and rearrangements by estimating the density of different repeat classes
313 and coding sequences in the chromosome regions associated with fusions and fissions and
314 comparing the densities to genomic regions not affected by rearrangements. We limited this
315 analysis to *L. reali* and *L. sinapis* where we could polarize the rearrangements as fissions or
316 fusions. In chromosome regions where fusions have occurred, there was a significant
317 enrichment of both LINEs and LTRs (p-value < 2.0×10^{-5} in both cases), and a significant
318 underrepresentation of SINEs (p-value < 2.0×10^{-5}) and rolling-circle TEs (p-value = 1.0×10^{-3}).
319 Similarly, there was a significant enrichment of LINEs and a reduction in SINEs and rolling-
320 circles (p < 2.0×10^{-5} in all cases) in chromosome ends in the lineages that lacked the fusion
321 (queries), but in these regions LTRs were not significantly enriched (Figure 6A,
322 Supplementary table 4). This shows that LTRs are more abundant where a fusion has
323 occurred compared to homologous regions in species where a fusion has not taken place. In
324 fission breakpoints in contrast, the only significant difference (p = 0.04) was found for rolling-
325 circles, which were underrepresented in fissioned as compared to non-fissioned
326 chromosomes (Figure 6B, Supplementary table 4).

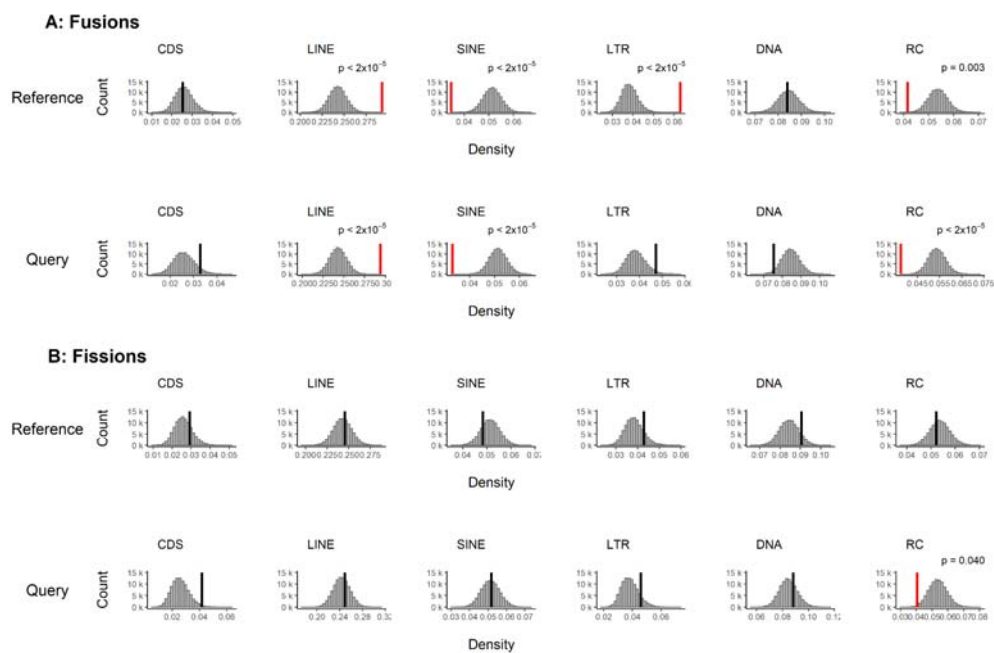


Figure 6. Composition of sequence elements in A) fusion and B) fission breakpoints as compared to the rest of the genomes for *L. reali* and *L. sinapis* (the outgroup *L. juvernica* was excluded from the analysis). Comparisons were performed separately for when the species were used as references or queries. The histograms show distributions of element densities generated by 100 k iterations of random genomic sampling with replacement. Vertical lines show mean density of elements in breakpoints, highlighted in red if significant and black if non-significant. FDR-adjusted p-values are indicated for significant tests. All p-values, means and standard deviations are reported in Supplementary table 4. CDS = coding sequence, LINE = long interspersed elements, SINE = short interspersed elements, LTR = long terminal repeats, DNA = DNA transposons, RC = rolling-circle TEs.

327 We found that the Asturian *L. sinapis* assembly contained more copies of the short telomeric
 328 repeat (TTAGG)_n compared to the in-house developed assemblies, and that these were
 329 interspersed with certain LINE families. We therefore assessed if increased LINE content in
 330 fused chromosome regions could be explained by the presence of telomere associated
 331 LINEs. Two classes of telomere associated LINEs had a higher frequency in telomeric
 332 regions than in the rest of the genome in the Asturian genome assembly (Fisher's exact test,
 333 fdr-adjusted p-value < 2.0*10⁻⁵⁷, Supplementary table 5). However, these LINE classes
 334 made up only 5.47% of the total LINE content in fused chromosome regions in *Leptidea*, and

335 LINEs in general were still significantly enriched (p-value = 8.0×10^{-4}) in those regions after
336 excluding this subset.

337

338 Discussion

339 Here we present the results from an integrative approach, where we combine genome
340 assembly and annotation with traditional linkage mapping, to characterize and quantify the
341 directions and frequencies of large scale chromosome rearrangements in *Leptidea*
342 butterflies. Our data showed lineage specific patterns of fissions, fusions (and potentially
343 some translocations) and unveiled considerable directional variation in karyomorph change
344 across species and populations. We also identified several segregating fission / fusion
345 polymorphisms in the *Leptidea* populations and characterized specific repeat classes
346 associated with chromosome regions involved in rearrangements. Since the extensive
347 rearrangements have occurred over a comparatively short time scale in *Leptidea* (Talla et
348 al., 2017), the system provides a unique opportunity for investigating the causes and
349 consequences of rapid karyotype change in recently diverged species.

350

351 Based on current chromosome number variation within *Leptidea* and the observation that the
352 inferred ancestral karyotype ($n = 31$) has been conserved across many divergent
353 lepidopteran lineages (de Vos et al., 2020; Robinson, 1971), a straightforward expectation
354 would be that *L. reali* ($n = 25 - 28$) and the northern populations of *L. sinapis* ($n = 28 - 29$)
355 have, apart from a few fusion events, mainly retained the ancestral lepidopteran
356 chromosome structures. This would mimic the rearrangements observed for *H. melpomene*,
357 where 10 fusions have reduced the chromosome number ($n = 21$) compared to the ancestral
358 karyotype (Davey et al., 2016). In line with this reasoning, the higher number of
359 chromosomes in *L. juvernica* ($n = 38 - 46$) and Iberian *L. sinapis* ($n \approx 53 - 55$) could simply

360 be a consequence of chromosomal fissions, as observed in the lycaenid genus *Lysandra*
361 (Pazhenkova & Lukhtanov, 2022). However, analogous to the organization of the genome
362 structure in *P. napi* and *P. rapae* (Hill et al., 2019), our analyses reveal considerably more
363 complex inter- and intra-chromosomal rearrangements in *Leptidea* than anticipated from
364 comparisons of chromosome counts. These results confirm previous findings of a dynamic
365 karyotype evolution in general in the species group (e.g. Dincă et al., 2011; Lukhtanov et al.,
366 2011; Šíčová et al., 2015; Yoshido et al., 2020) and extends them by characterizing the
367 specific chromosome rearrangements in detail and quantifying the differences in fission and
368 fusion rates in different *Leptidea* species and populations. Despite the rather complex
369 patterns of restructuring observed, we found some general trends of karyotype change
370 between the species. For *L. reali* and the Swedish *L. sinapis* population, most species-
371 specific chromosomes have been formed from fusions of chromosomes that segregate
372 independently in Catalan *L. sinapis*. In Catalan *L. sinapis* on the other hand, lineage specific
373 chromosomes have mainly formed through fissions of larger ancestral chromosomes. Since
374 *L. juvernica* was used as an outgroup in the analysis, we could not infer direction in this
375 lineage. However, comparisons with more divergent lepidopteran species suggest that both
376 fissions and fusions have occurred at a high rate also in *L. juvernica*.

377

378 Our analyses show that the synteny blocks are short between *Leptidea* and the inferred
379 ancestral karyotype - typically less than 1 Mb, which translates to 12 - 15 blocks per
380 chromosome. Albeit less extensive, such a pattern has also been observed in *Pieris* sp. and
381 has been suggested to reflect a history of recurrent reciprocal chromosome translocations
382 (Hill et al., 2019). The synteny comparison between *Leptidea* species and *B. mori* showed
383 that not a single chromosome in any *Leptidea* species has retained both chromosome ends
384 and that only a minor fraction (~ 12 - 19%) have retained one of the ancestral ends. We also
385 detect few signs of translocations and the high degree of synteny fragmentation in *Leptidea*
386 is therefore probably a consequence of recurrent fissions and fusions in different
387 chromosome regions and between different chromosome pairs, respectively.

388

389 The short synteny blocks also show that extensive chromosomal restructuring has occurred
390 in the ancestral lineage of the *Leptidea* species included in our analyses and continued at a
391 high rate in all species. Although we did not have data for all species in the genus, the
392 inferred ancestral karyomorph of the analyzed species (n ~ 50) in combination with the high
393 and variable chromosome numbers in more divergent *Leptidea* species - *L. amurensis* (n =
394 59 - 61), *L. duponcheli* (n = 102 - 104) and *L. morsei* (n = 54) (Robinson, 1971; Šíchová et
395 al., 2016) - suggest that a high chromosome rearrangement rate is ubiquitous in wood
396 whites. In *L. reali* for example, the chromosome count has decreased to n = 26 in 1 - 2 My
397 since the split from *L. sinapis* (Talla et al., 2017). Even more striking is the rate of change in
398 *L. sinapis* where chromosome counts range from n = 27 - 55 between recently diverged
399 populations. This translates to a chromosome number evolutionary rate in both *L. sinapis*
400 and *L. reali* that has been considerably faster than in for example *H. melpomene*, where 10
401 chromosome fusions have occurred over the last six million years (Davey et al., 2016).
402 Additional support for an extreme rearrangement rate in the genus comes from the
403 observations that several intraspecific fission / fusion polymorphisms are currently
404 segregating within the different species (see also Lukhtanov et al., 2011; Šíchová et al.,
405 2015) and that incomplete lineage sorting and / or recurrent rearrangements involving the
406 same chromosome regions have been frequent in *Leptidea* historically.

407

408 Lepidoptera has traditionally been viewed as having a conserved genomic synteny.
409 However, recent studies (Hill et al., 2019; Yoshido et al., 2020) and the results presented
410 here add some doubt to this view. As mentioned above, an elevated rate of chromosome
411 rearrangements has for example also been observed in the *Pieris napi* / *rapae* lineage (Hill
412 et al., 2019), which belongs to the same family as *Leptidea* (Pieridae), but the two genera
413 diverged approximately 80 Mya (Espeland et al., 2018) and our synteny analysis clearly
414 show that the rearrangements have occurred independently. Given the limited availability of
415 high-contiguity genome assemblies and / or high-resolution linkage maps, a more holistic

416 view of inter- and intra-chromosomal rearrangement rates will have to await broader
417 taxonomic sampling. Still, we can ask why some lepidopteran taxa are extremely conserved
418 in terms of karyotype and synteny, while other lineages have accumulated a large number of
419 fissions, fusions and translocations, and also why some chromosomes are more conserved
420 than others. Holocentricity and female achiasmy may facilitate segregation and retention of
421 polymorphic chromosomes (Melters et al., 2012), and consequently accelerate genome
422 restructuring. However, a recent phylogenetic overview in insects showed that karyotype
423 evolution is not accelerated in clades with holocentric chromosomes as compared to
424 monocentric, although Lepidoptera appears to be an exception with higher rates of both
425 fissions and fusions (Ruckman et al., 2020). Inverted (post-reductional) meiosis is another
426 mechanism proposed to be important for mitigating the negative effects of chromosomal
427 heterozygosity (Lukhtanov et al., 2018). Within Lepidoptera, this phenomenon has been
428 observed in *L. sinapis* (Lukhtanov et al., 2018) and facultatively in *B. mori* (Banno et al.,
429 1995) and *Polyommatus poseidonides* (Lukhtanov et al., 2020), but because of its
430 association with holocentric chromosomes (Melters et al., 2012) it could potentially be more
431 widespread. However, why do we not observe an elevated rate of chromosome
432 rearrangements in butterflies and moths in general? *Bombyx mori*, for example, has a similar
433 repeat density as *Leptidea* (Tang et al., 2021) and shares the potential for inverted meiosis
434 (Banno et al., 1995). Still *B. mori*, and the majority of lepidopteran taxa with chromosome
435 structure information, have retained the ancestral lepidopteran karyotype (Ahola et al., 2014;
436 Pringle et al., 2007). One option is that chromosome rearrangements are dependent on the
437 presence of specific features that generate *de novo* rearrangement mutations - i.e. that the
438 rate of structural change is mutation limited. Within *Leptidea* for example, a relatively recent
439 burst of transposable element activity has occurred (Talla et al., 2017). This increased
440 activity of certain TE classes could potentially be an important driver of genomic
441 restructuring. We found for example increased LINE and LTR density in fused chromosome
442 regions. Previous data suggest that LINEs make up a considerable portion of the telomere
443 regions in Lepidoptera (Okazaki et al., 1995; Takahashi et al., 1997), but the specific class

444 we could associate with telomeres in *Leptidea* could not explain the general enrichment of
445 LINEs in fused regions. LINEs have previously been associated with rearrangements in
446 monocentric organisms, for example bats (Sotero-Caio et al., 2015) and gibbons (Carbone
447 et al., 2014). Enrichment of LINEs and LTRs was similarly shown to occur in synteny
448 breakpoints within the highly rearranged genome of the aphid *Myzus persicae* (Mathers et
449 al., 2021), although in this case several other classes of TEs were also overrepresented. A
450 plausible explanation is that an increase in ectopic recombination between similar copies of
451 specific TE repeat classes located on different chromosomes (Almojil et al., 2021) can lead
452 to rearrangements, but only in species where these specific classes have proliferated
453 recently. In *Heliconius*, for example, there is a higher density of TEs in general in
454 chromosome fusion points (Cicconardi et al., 2021). Here, we found that the enrichment of
455 LINEs was significant both in species / regions where a chromosome fusion has taken place
456 and in homologous chromosome regions in species where the fusion event has not
457 occurred. This shows that the density of LINEs has been higher in chromosome regions
458 where fusions have occurred rather than accumulating in the regions after the fusion event
459 and indicates that recently proliferated LINE families could play an important role for
460 rearrangements in *Leptidea*. However, we found no association between any of the
461 investigated genomic features and chromosome fission events which indicates that
462 chromosome breakage depends on a mechanism that we could not pick up with our data.

463

464 Although *Leptidea* has the most rearranged sex chromosomes of any Lepidopteran species
465 described so far (Yoshido et al., 2020), our synteny analysis showed that the Z
466 chromosomes are considerably more structurally conserved than the autosomes. In
467 particular Z2, which is the only chromosome that has been completely conserved since the
468 split of the *Leptidea* species. The gene content of the ancestral Z chromosome has also
469 been maintained, although the gene order has been highly reshuffled from the ancestral
470 state. A similar situation of sex chromosome conservation in the face of extensive genome
471 restructuring was recently shown in the aphid *M. persicae* (Mathers et al., 2021) and the Z

472 chromosome is highly conserved in Lepidoptera (Fraïsse et al., 2017; Sahara et al., 2012),
473 even in rearranged genomes (Hill et al., 2019), but several cases of fusions with autosomes
474 have been documented (Hill et al., 2019; Mongue et al., 2017; Nguyen et al., 2013). In
475 systems where one sex chromosome is degenerated, for example the W chromosomes in
476 lizards (Iannucci et al., 2019), snakes (Rovatsos et al., 2015) and butterflies (Lewis et al.,
477 2021), the other sex-chromosome (here Z-chromosomes) is often highly conserved. One
478 potential explanation for this is that translocation of genes with male-biased expression from
479 the Z chromosome to an autosome likely would have deleterious effects in females (Vicoso,
480 2019). It has also been proposed that selection for maintaining linkage of genes with sex-
481 biased expression can be a strong stabilizing force, as seen for example in birds (Nanda et
482 al., 2008). Accumulation of male biased genes on the Z chromosome, as has been observed
483 in many lepidopteran species (Arunkumar et al., 2009; Mongue & Walters, 2018) including *L.*
484 *sinapis* (Höök et al., 2019), can therefore be a potential reason for the much more conserved
485 Z chromosomes. The fact that the Z chromosome only recombines and spends relatively
486 more time in male butterflies (Turner & Sheppard, 1975) should further strengthen this
487 linkage. Translocation of genes from the sex chromosomes might also be selected against if
488 it alters expression levels regulated by dosage compensation mechanisms, which has been
489 observed in *L. sinapis* (Höök et al., 2019).

490

491 Conclusion

492 Here we present female and male genome assemblies for three different *Leptidea* species
493 and develop detailed linkage maps for two populations of *L. sinapis*. Synteny analysis
494 revealed one of the most dramatic and rapid cases of chromosome evolution presented so
495 far. The genus not only has one of the most variable intra- and interspecific chromosome
496 numbers, but also, as shown here, potentially the most rearranged genomes across
497 Lepidoptera. Our data suggests that fissions and fusions have been the main cause of the
498 restructuring and that several rearrangement polymorphisms still segregate in the different

499 species and populations. We further find an association between LINEs and LTR elements
500 and fusion breakpoints which should be explored in more depth in future studies. The results
501 presented here add another example of extensive genome reshuffling in Lepidoptera, which
502 shows that the karyomorph does not necessarily predict the extent of chromosome
503 rearrangements in a species.

504

505 Methods

506 *Samples*

507 Mated adult females of *L. sinapis* (Sweden and Catalonia), *L. reali* (Catalonia) and *L.*
508 *juvernica* (Sweden) were sampled in the field 2019 and kept in the lab for egg laying. One
509 male and one female offspring from each dam were sampled at the chrysalis stage and flash
510 frozen in liquid nitrogen. Each sample was divided in two aliquots to allow for generation of
511 both a 10X Genomics Chromium Genome- and a Dovetail HiC-library from each individual.
512 For 10X sequencing, DNA was extracted using a modified high molecular weight salt
513 extraction method (Aljanabi & Martinez, 1997). Tissues were homogenized for HiC
514 sequencing using a mortar and pestle in liquid nitrogen and sent to the National Genomics
515 Infrastructure (NGI, Stockholm) for library preparation and sequencing.

516

517 *Sequencing and assembly*

518 Library preparations, sequencing and genome assembly was performed by NGI Stockholm
519 using the Illumina NovaSeq6000 technology with 2 x 151 bp read length. 10X linked reads
520 were assembled with 10X Genomics Supernova v. 2.1.0 (Weisenfeld et al., 2017). HiC reads
521 were processed with Juicer v. 1.6 (Durand et al., 2016a) and assemblies were scaffolded
522 with 3DDNA v.180922 (Dudchenko et al., 2017). Resulting assemblies were corrected in
523 several consecutive steps with Juicebox v. 1.11.08 (Durand et al., 2016b). First, all obvious
524 scaffolding errors were corrected using the HiC contact information. Next, linkage

525 information (see subheading “Linkage maps”) was used to identify and correct technical
526 inversions and translocations in the *L. sinapis* assemblies. Finally, we used pairwise
527 alignments (see Genome alignments) between i) the male and female from each respective
528 population, and ii) all assemblies, including an assembly of an Asturian *L. sinapis* individual
529 from the Darwin Tree of Life (DToL) initiative (Lohse et al., 2022), and used visual inspection
530 to detect deviating scaffold orders or orientations. Manual corrections were done in cases
531 when the orientation was not in conflict with the HiC-signal (Supplementary figure 1). After
532 manual curation, the number of chromosome sized scaffolds for each assembly (Swedish *L.*
533 *sinapis* n = 28 - 29, Catalan *L. sinapis* n = 52, *L. reali* n = 26, *L. juvernica* n = 42 - 43) was
534 within the expected karyotype range (Dincă et al., 2011; Lukhtanov et al., 2011; Šíchová et
535 al., 2015) and these scaffolds contained the majority of the total sequence content (Table 1,
536 Supplementary figure 1 and 2). In addition, collinearity between male and female assemblies
537 improved after manual curation (Supplementary figure 12). Redundant scaffolds (100%
538 identical duplicates and scaffolds contained within others) were removed using ‘dedupe.sh’
539 in BBTools v. 38.61b (Bushnell, 2019). The core gene completeness of the different
540 assemblies was assessed with BUSCO v. 3.0.2 (Simão et al., 2015) using the insecta_odb9
541 data set. The percent of complete BUSCO insect orthologs ranged between 93.4% in *L. reali*
542 male to 95.0% in *L. juvernica* male (Table 1, Supplementary table 1). Potential contaminant
543 scaffolds were identified and removed using BlobTools v. 1.1.1 (Laetsch & Blaxter, 2017).
544

545 **Linkage map**

546 *Sampling, DNA-extraction and sequencing protocol*

547 Offspring from wild caught females from two populations of *L. sinapis* with different
548 karyotypes (Sweden n = 28 - 29; Catalonia n = 53 - 55) were reared on cuttings of *Lotus*
549 *corniculatus*. The pedigrees consisted of 6 dams and 184 and 178 offspring from the
550 Swedish and Catalan population, respectively (Supplementary table 6). The offspring were
551 sampled at larval instar V, snap frozen in liquid nitrogen and stored at -20°C. DNA-

552 extractions from caudal abdominal segments were performed with a modified Phenol-
553 Chloroform extraction (batch1; Sambrook & Russell, 2006) or high salt extraction (batch2;
554 Aljanabi & Martinez, 1997) after standard Proteinase-K digestion overnight. The amount and
555 quality of the DNA was analyzed with Nanodrop (Thermo Fisher Scientific) and Qubit
556 (Thermo Fisher Scientific). The DNA was digested with the *EcoR1* enzyme according to the
557 manufacturer's protocol, using 16 hours digestion time (Thermo Fisher Scientific). The
558 efficiency of the digestion was determined by visual inspection of the fragmentation using gel
559 electrophoresis (1% agarose gel). The fragmented DNA samples were sent for RAD-seq
560 library preparation and paired-end sequencing on Illumina HiSeq2500 (batch 1) and
561 NovaSeq600 (batch 2) at the National Genomics Infrastructure, SciLife, Stockholm.

562

563 *Data processing*

564 The quality of the raw reads was initially assessed with FastQC (Andrews, 2010). Duplicate
565 removal and quality filtering were performed with clone_filter and process_radtags from
566 Stacks2 (Catchen et al., 2013). We applied the quality filtering options -q to filter out reads
567 with > phred score 10 (90% probability of correct base called) in windows 15% of the length
568 of the read, -c to remove all reads with unassigned bases, and --disable_rad_chec to keep
569 reads without complete RAD-tags. All reads were truncated to 120 bp. The filtered reads
570 were mapped to the male genome assembly from each population using bwa mem with
571 default options, and sorted with samtools sort (Li et al., 2009). The bam-files were further
572 filtered with samtools view -q 30 option and a custom script to only retain reads with unique
573 mapping positions. The mapping coverage was analyzed with Qualimap (Okonechnikov et
574 al., 2016) and individual coverage was visualized as mean coverage per chromosome
575 divided by mean coverage per individual. The sex of offspring was set as female if the
576 normalized coverage on the Z1- and Z2-chromosomes was < 75% compared to the
577 autosomes. We used Samtools mpileup for variant calling with minimum mapping quality (-q)
578 10 and minimum base quality (-Q) 10 (Li, 2011). The variants were converted to likelihoods
579 using Pileup2Likelihoods in LepMap3 with default settings (Rastas, 2017), minimum

580 coverage 3 per individual (minCoverage = 3) and 30% of the individuals allowed to have
581 lower coverage than minimum coverage (numLowerCoverage = 0.3). To verify that the
582 pedigree was correct, the relatedness coefficients of the samples were estimated with the
583 module IBD in LepMap3 using 10% of the markers and a multiple dimensional
584 scaling/principal coordinate analysis based on a distance matrix inferred with Tassel 5 v.
585 20210210 (Bradbury et al., 2007).

586

587 *Linkage map construction*

588 LepMap3 was used to construct the linkage maps (Rastas, 2017). Informative parental
589 markers were called with module ParentCall using default values, except that non-
590 informative markers were removed and we applied the setting zLimit = 2 to detect markers
591 segregating as sex chromosomes. This module also uses genotype likelihood information
592 from the offspring to impute missing or erroneous parental markers. Markers that did not
593 map to the chromosome-size scaffolds in the physical assembly were removed. The module
594 Filtering2 was applied to remove markers with high segregation distortion (dataTolerance =
595 0.00001) and markers that were missing in more than 30% of the individuals in each family
596 (missingLimit = 0.3). In addition, only markers present in at least five families were retained
597 (familyInformativeLimit = 5). The markers were binned over stretches of 10 kb with a custom
598 script and binned markers with more than five SNPs per bin were removed. The module
599 OrderMarkers2 with the option outputPhasedData = 4 was used to phase all binned data.
600 The final binning and filtering resulted in 3,237 and 4,207 retained markers in the Swedish
601 and Catalan pedigree, respectively.

602

603 The markers were assigned to linkage groups using the module SeparateChromosomes2,
604 with an empirically estimated lodLimit. The lodLimit is the threshold for the logarithm of the
605 odds that two markers are inherited together (LOD-score), i.e. belonging to the same linkage
606 group. We evaluated a range of lodLimits (1 - 30) and finally set it to 10 for the Catalan and
607 12 for the Swedish families - settings that resulted in approximately the number of linkage

608 groups expected from karyotype data (50 linkage groups in the Catalan and 23 linkage
609 groups in the Swedish families, respectively). To assign additional unlinked markers to the
610 linkage groups, JoinSingles was run with IodLimits 5 for the Catalan map and 8 for the
611 Swedish. Since butterflies have female heterogamety and female achiasmy, the three
612 different Z-chromosomes were clustered in one linkage group and had to be split in separate
613 linkage groups manually (based on information from the physical genome assemblies). To
614 correct for interference and multiple recombination events per linkage group we applied the
615 Kosambi correction. To account for female achiasmy, the recombination rate in females was
616 set to zero (recombination2 = 0). The linkage maps were refined by manually removing non-
617 informative markers at the ends of each map. The trimmed map was re-evaluated with
618 OrderMarkers with the options evaluateOrder and improveOrder = 1. Remaining unlinked
619 markers at map ends were manually removed after visual inspection and the maps were
620 once again re-evaluated with OrderMarkers. The genetic distances and marker orders were
621 compared to the physical positions along each chromosome and the physical coordinates for
622 potential rearrangements were used for re-evaluation of the HiC-maps (Figure 1). The
623 collinearity of the genetic and physical maps was assessed using Spearman's rank
624 correlation.

625 *Read mapping*
626 10X raw reads were first processed with Long ranger basic v. 2.2.2 (Marks et al., 2019).
627 Reads were then trimmed for low quality bases and adapters with Cutadapt v. 2.3 (Martin,
628 2011) in TrimGalore v. 0.6.1 (Krueger, 2019) using the NovaSeq filter (--nextseq 30) and
629 discarding trimmed reads shorter than 30 bp. Fastqscreen v. 0.11.1 (Wingett & Andrews,
630 2018) was used to screen and filter libraries from common contaminants (*A. thaliana*, *D.*
631 *melanogaster*, *E. coli*, *S. cerevisiae*, *H. sapiens*, *C. familiaris*, *M. musculus*, *Wolbachia* and
632 *L. corniculatus*, downloaded from NCBI 2021-03-05). Reads were mapped with BWA mem v.
633 0.7.17 (Li, 2013) resulting in a high mapping rate across all assemblies (98.0 - 98.6 %; Table
634 1). Mapped reads were then filtered for supplementary and secondary alignments with a

635 custom script, and low-quality alignments (mapq < 30) with samtools v1.10 (Li et al., 2009).
636 Duplicate reads were removed using MarkDuplicates in GATK v. 4.1.1.0 (McKenna et al.,
637 2010). Resulting read mappings were assessed with samtools flagstats (Li et al., 2009) and
638 QualiMap v. 2.2 (Okonechnikov et al., 2016).

639

640 *MtDNA*

641 Circularized mitochondrial genomes for each sample were assembled de novo from
642 processed 10X reads using NOVOplasty v. 4.2 (Dierckxsens et al., 2017) with the *COX1*
643 gene from *Leptidea morsei* as seed (downloaded from NCBI 2020-08-29). The mitochondrial
644 genomes were annotated with MITOS (Bernt et al., 2013), using custom scripts to set the
645 gene *TRNM* as starting position. To identify and remove partial mtDNA scaffolds from the
646 nuclear genome assemblies, we aligned the mtDNA genomes to the assemblies with
647 nucmer in MUMmer v. 4.0.0rc1 (Marçais et al., 2018) using default settings and filtering the
648 output with delta-filter -g. Scaffolds aligning by > 95% of their length and with > 95% identity
649 were filtered out using a custom script. After filtering away identified partial mtDNA scaffolds
650 we reintroduced the mtDNA as a separate scaffold to each assembly.

651

652 *Sex chromosome identification*

653 Sex chromosomes were identified by homology and read coverage. We used gene synteny
654 (see synteny analysis) between *B. mori* and the sequenced *Leptidea* species to verify
655 previously characterized sex and neo-sex chromosomes (Yoshido et al., 2020). As an
656 independent validation we analyzed read depth (see read mapping) for chromosome sized
657 scaffolds across the female and male assemblies with QualiMap v. 2.2 (Okonechnikov et al.,
658 2016). For scaffolds identified as sex chromosomes, the mean read coverage in females
659 ranged between 49.36 - 74.44% of mean assembly coverage (Supplementary table 7,
660 Supplementary figure 18). Sex chromosomes were also verified visually in non-normalized
661 HiC heatmaps, where female samples had a clearly reduced contact between identified sex

662 chromosomes and autosomes (Supplementary figure 1) as compared to the background
663 noise.

664

665 *Gene and repeat annotation*

666 Repeat libraries were generated *de novo* with RepeatModeler v. 1.0.11 (Smit & Hubley,
667 2017) using default settings. Repeat families classified as unknown by RepeatModeler were
668 additionally screened against Repbase (Jurka, 1998) using CENSOR (Kohany et al., 2006)
669 with the options 'sequence source - Eukaryota' and 'report simple repeat'. The highest
670 scoring hit for each query was integrated with the RepeatModeler output using custom
671 scripts. Repeats were then annotated and quantified using RepeatMasker v. 4.1.0 (Smit et
672 al., 2019). Genes were annotated for the male genome assemblies of each species with the
673 MAKER pipeline v. 3.01.04 (Cantarel et al., 2008). First, both translated protein and coding
674 nucleotide sequences were used as input evidence. Protein sequences were a combination
675 of previous *L. sinapis* annotations (Talla et al., 2019), reviewed Lepidoptera proteins from
676 uniprot (downloaded 2021-04-02) and a set of Lepidoptera core orthologs from Kawahara &
677 Breinholt, 2014. Coding sequences were a combination of *L. sinapis* (Talla et al., 2019) and
678 *L. juvernica* (Yoshido et al., 2020) transcripts. In addition, the output of RepeatModeler was
679 used to mask repeat sequences within MAKER. Resulting gene models were used to train
680 *ab initio* gene predictors in snap (Korf, 2004) and Augustus v. 3.4.0 (Stanke et al., 2008).
681 The gff-file generated in the first round and the gene predictors were then used jointly in a
682 second round of gene prediction. The number of resulting annotations ranged between 15
683 689 - 17 229 and were of expected quality and size (Supplementary table 8, Supplementary
684 figures 19 and 20). The final gene models were functionally annotated with Interproscan v.
685 5.30-69.0 (Jones et al., 2014) and blast searches against Swiss-Prot.

686

687 *Synteny analysis*

688 Gene synteny was compared between the male assemblies from each of the sequenced
689 *Leptidea* species and the two reference species *Bombyx mori* and *Melitaea cinxia*, and in

690 addition *Pieris napi* (assemblies and annotations downloaded from NCBI 2021-04-25). First,
691 reciprocal protein alignments were generated with blastp. The blast output was then trimmed
692 to include the top five best hits per query. Finally, synteny blocks were built with MCScanX
693 (Wang et al., 2012) using default settings but restricting the maximum gene gap size to 10 to
694 reduce the amount of overlapping synteny blocks. The results were visualized with Synvisio
695 (Bandi & Gutwin, 2020) and Circos v. 0.69-9 (Krzywinski et al., 2009).

696

697 *Genome alignments*

698 To guide manual curation, estimate collinearity and detect rearrangements, all assemblies
699 were aligned to the male assembly of each respective species with nucmer in MUMmer v.
700 4.0.0rc1 (Marçais et al., 2018), using default settings. Alignments were restricted to the
701 chromosome sized scaffolds of each assembly. The resulting alignments were filtered with
702 delta-filter -1 to get 1-to-1 alignments including rearrangements. Male to female alignments
703 for each species were visualized with dotplots using a modified version of the script
704 'mummerCoordsDotPlotly.R' from dotPlotly (Poorten, 2018).

705

706 *Rearrangement analysis*

707 Large scale rearrangements were identified from breakpoints in alignments, when queries
708 changed from aligning against one reference scaffold to another. First, blocks of consecutive
709 alignments (> 90% similarity) between the homologous scaffolds were built using a custom
710 script, removing singleton queries against other scaffolds and only keeping blocks > 100 kb.
711 Rearrangements were then classified using a phylogenetic approach, by finding unique or
712 shared breakpoints between assemblies when aligned against the same reference using
713 bedtools v. 2.29.2 (Quinlan & Hall, 2010). Each male assembly was separately used as
714 reference, complemented by the alignment of the female assembly of the same species as
715 an additional control for interspecific variation. Unique breakpoints were called as fissions in
716 the query species while breakpoints shared by all query species were called as fusions in
717 the reference. Following the same logic, we searched for shared breakpoints between all

718 possible combinations of species pairs to find potential cases of incomplete lineage sorting,
719 reuse of breakpoints or rearrangements in ancestral *L. sinapis* (shared by both populations).
720 The output of each separate comparison was checked and manually curated for any
721 discrepancies resulting from using different references. In addition, based on the identified
722 breakpoints, we quantified potential translocations as any case where two chromosomes in
723 one species contained the same combination of parts from two chromosomes in another
724 species (reciprocal) and cases where one chromosome had one alignment block flanked by
725 two blocks from one other chromosome in another species (non-reciprocal).

726

727 *Breakpoint content analysis*

728 The composition of genetic elements in chromosome breakpoints was analyzed by
729 comparing the observed mean density (here defined as proportion of base pairs) of coding
730 sequence and different transposable element (TE) classes to random resampling
731 distributions taken from the rest of the genomes. TEs from the same category and with
732 overlapping coordinates were merged before analysis. Resampling (with replacement, 100 k
733 iterations) was performed by taking random non-overlapping windows of the same size and
734 number as identified fusions or fissions, and calculating the mean density of sequence
735 elements across the sampled windows. The empirical means were compared to the
736 generated resampling distributions using a two-tailed significance test. The false discovery
737 rate was controlled for by adjusting p-values with the Benjamini-Hochberg method
738 (Benjamini & Hochberg, 1995). Fusion and fission breakpoints were analyzed separately,
739 only including events identified in the ingroup species (*L. sinapis* and *L. reali*) and excluding
740 cases with ambiguous polarity. To account for variation in breakpoint size, breakpoints were
741 standardized to 100 kb around their midpoint. In addition, separate tests were made for
742 corresponding homologous regions in the alignment queries. Since there is no shared
743 midpoint coordinate between two query chromosomes flanking a breakpoint, we instead
744 selected two 50 kb windows starting from the last query coordinate of each alignment block
745 and extending towards a theoretical point of breakage. The terminal 50 kb were selected in

746 cases where windows extended beyond the end of the query scaffold. Since the same set of
747 query fissions were scored against two references and not necessarily overlapped, we
748 selected the breakpoints with the coordinates closest to the terminal ends. Similarly, when
749 the same chromosome end was associated with two different fusion events, we selected the
750 outermost coordinates to represent the region. When analyzing query sequences, we
751 excluded internal breakpoints, defined as occurring > 1 Mb from the chromosome terminal
752 ends, as these cases indicate either fissions followed by subsequent fusions (not necessarily
753 representative of a fission) or that different fusions have occurred in the reference and the
754 query and are therefore already counted when each respective species is used as reference.
755 The analysis was performed using bedtools v2.29.2 (Quinlan & Hall, 2010) and custom
756 scripts.

757

758 Fusion breakpoints were investigated for the presence and accumulation of telomere
759 associated LINE elements. Putative telomeric LINEs were first identified in the terminal 250
760 kb of scaffolds of the DToL *L. sinapis* assembly (Lohse et al., 2022). Enrichment of specific
761 LINEs in telomeric regions were then called with Fisher's exact test using an alpha level of
762 0.05 and adjusting p-values with the Benjamini-Hochberg method (Benjamini & Hochberg,
763 1995), and requiring at least the same count of each element in telomeric regions as the
764 number of telomeres ($n = 96$) and presence in telomeric regions of at least half of the
765 chromosomes. Homologous LINEs in the other assemblies (Swedish + Catalan *L. sinapis*
766 and *L. reali*) were then identified with reciprocal blast alignments, keeping all hits as putative
767 telomere specific LINEs. Finally, accumulation was quantified by calculating the summed
768 fraction of putative telomeric LINEs out of the total LINE density in fusion breakpoints. All
769 statistical tests were performed in R (R Core Team, 2019) unless otherwise noted.

770 Competing interests statement

771 The authors declare no competing interests.

772

773 Data availability

774 All raw sequence data have been deposited at the European Nucleotide Archive under
775 accession ENAXXXX. All in-house developed scripts and pipelines are available in GitHub
776 (<https://github.com/EBC-butterfly-genomics-team>).

777 Acknowledgements

778 This work was funded by the Swedish Research Council (VR research grant #019-04791 to
779 N.B.). The authors acknowledge support from the National Genomics Infrastructure in
780 Stockholm funded by Science for Life Laboratory, the Knut and Alice Wallenberg Foundation
781 and the Swedish Research Council, and SNIC/Uppsala Multidisciplinary Center for
782 Advanced Computational Science for assistance with massively parallel sequencing and
783 access to the UPPMAX computational infrastructure. We also acknowledge SciLifeLab in
784 Uppsala for long-term bioinformatics support via the WABI initiative. R.V. was supported by
785 project PID2019-107078GB-I00, funded by Ministerio de Ciencia e Innovación
786 (MCIN)/Agencia Estatal de Investigación (AEI) 10.13039/501100011033.

787

788 References

789 Ahola, V., Lehtonen, R., Somervuo, P., Salmela, L., Koskinen, P., Rastas, P., Välimäki, N.,
790 Paulin, L., Kvist, J., Wahlberg, N., Tanskanen, J., Hornett, E. A., Ferguson, L. C.,
791 Luo, S., Cao, Z., de Jong, M. A., Duplouy, A., Smolander, O.-P., Vogel, H., ...
792 Hanski, I. (2014). The Glanville fritillary genome retains an ancient karyotype and

793 reveals selective chromosomal fusions in Lepidoptera. *Nature Communications*, 5(1),
794 4737. <https://doi.org/10.1038/ncomms5737>

795 Aljanabi, S. M., & Martinez, I. (1997). Universal and rapid salt-extraction of high quality
796 genomic DNA for PCR-based techniques. *Nucleic Acids Research*, 25(22), 4692–
797 4693. <https://doi.org/10.1093/nar/25.22.4692>

798 Almojil, D., Bourgeois, Y., Falis, M., Hariyani, I., Wilcox, J., & Boissinot, S. (2021). The
799 Structural, Functional and Evolutionary Impact of Transposable Elements in
800 Eukaryotes. *Genes*, 12(6), 918. <https://doi.org/10.3390/genes12060918>

801 Andrews, S. (2010). *Babraham Bioinformatics—FastQC A Quality Control tool for High*
802 *Throughput Sequence Data*.
803 <https://www.bioinformatics.babraham.ac.uk/projects/fastqc/>

804 Arunkumar, K. P., Mita, K., & Nagaraju, J. (2009). The Silkworm Z Chromosome Is Enriched
805 in Testis-Specific Genes. *Genetics*, 182(2), 493–501.
806 <https://doi.org/10.1534/genetics.108.099994>

807 Bandi, V., & Gutwin, C. (n.d.). *Interactive Exploration of Genomic Conservation*. 10.

808 Banno, Y., Kawaguchi, Y., Koga, K., & Doira, H. (1995). Postreductional meiosis revealed in
809 males of the mutant with chromosomal aberration “T (23;25) Nd” of the silkworm
810 *Bombyx mori*. *The Journal of Sericultural Science of Japan*, 64(5), 410–414.
811 <https://doi.org/10.11416/kontyushigen1930.64.410>

812 Belyayev, A. (2014). Bursts of transposable elements as an evolutionary driving force.
813 *Journal of Evolutionary Biology*, 27(12), 2573–2584.
814 <https://doi.org/10.1111/jeb.12513>

815 Benjamini, Y., & Hochberg, Y. (1995). Controlling the False Discovery Rate: A Practical and
816 Powerful Approach to Multiple Testing. *Journal of the Royal Statistical Society.*
817 *Series B (Methodological)*, 57(1), 289–300.

818 Bernt, M., Donath, A., Jühling, F., Externbrink, F., Florentz, C., Fritzsch, G., Pütz, J.,
819 Middendorf, M., & Stadler, P. F. (2013). MITOS: Improved de novo metazoan

820 mitochondrial genome annotation. *Molecular Phylogenetics and Evolution*, 69(2),
821 313–319. <https://doi.org/10.1016/j.ympev.2012.08.023>

822 Blackmon, H., Justison, J., Mayrose, I., & Goldberg, E. E. (2019). Meiotic drive shapes rates
823 of karyotype evolution in mammals. *Evolution*, 73(3), 511–523.
824 <https://doi.org/10.1111/evo.13682>

825 Boggs, C. L., Watt, W. B., Ehrlich, P. R., Ehrlich, P. R., & Ehrlich, P. R. (2003). *Butterflies:*
826 *Ecology and Evolution Taking Flight*. University of Chicago Press.

827 Bradbury, P. J., Zhang, Z., Kroon, D. E., Casstevens, T. M., Ramdoss, Y., & Buckler, E. S.
828 (2007). TASSEL: Software for association mapping of complex traits in diverse
829 samples. *Bioinformatics*, 23(19), 2633–2635.
830 <https://doi.org/10.1093/bioinformatics/btm308>

831 Brown, K. S., Jr, Von Schoultz, B., & Suomalainen, E. (2004). Chromosome evolution in
832 Neotropical Danainae and Ithomiinae (Lepidoptera). *Hereditas*, 141(3), 216–236.
833 <https://doi.org/10.1111/j.1601-5223.2004.01868.x>

834 Bushnell, B. (2019). *BBMap*. SourceForge. <https://sourceforge.net/projects/bbmap/>

835 Cantarel, B. L., Korf, I., Robb, S. M. C., Parra, G., Ross, E., Moore, B., Holt, C., Sánchez
836 Alvarado, A., & Yandell, M. (2008). MAKER: An easy-to-use annotation pipeline
837 designed for emerging model organism genomes. *Genome Research*, 18(1), 188–
838 196. <https://doi.org/10.1101/gr.6743907>

839 Carbone, L., Alan Harris, R., Gnerre, S., Veeramah, K. R., Lorente-Galdos, B., Huddleston,
840 J., Meyer, T. J., Herrero, J., Roos, C., Aken, B., Anacleto, F., Archidiacono, N.,
841 Baker, C., Barrell, D., Batzer, M. A., Beal, K., Blancher, A., Bohrson, C. L., Brameier,
842 M., ... Gibbs, R. A. (2014). Gibbon genome and the fast karyotype evolution of small
843 apes. *Nature*, 513(7517), 195–201. <https://doi.org/10.1038/nature13679>

844 Catchen, J., Hohenlohe, P. A., Bassham, S., Amores, A., & Cresko, W. A. (2013). Stacks:
845 An analysis tool set for population genomics. *Molecular Ecology*, 22(11), 3124–3140.
846 <https://doi.org/10.1111/mec.12354>

847 Cicconardi, F., Lewis, J. J., Martin, S. H., Reed, R. D., Danko, C. G., & Montgomery, S. H.
848 (2021). Chromosome Fusion Affects Genetic Diversity and Evolutionary Turnover of
849 Functional Loci but Consistently Depends on Chromosome Size. *Molecular Biology*
850 and Evolution, 38(10), 4449–4462. <https://doi.org/10.1093/molbev/msab185>

851 Davey, J. W., Chouteau, M., Barker, S. L., Maroja, L., Baxter, S. W., Simpson, F., Merrill, R.
852 M., Joron, M., Mallet, J., Dasmahapatra, K. K., & Jiggins, C. D. (2016). Major
853 Improvements to the *Heliconius melpomene* Genome Assembly Used to Confirm 10
854 Chromosome Fusion Events in 6 Million Years of Butterfly Evolution. *G3: Genes,*
855 *Genomes, Genetics*, 6(3), 695–708. <https://doi.org/10.1534/g3.115.023655>

856 de Vos, J. M., Augustijnen, H., Bätscher, L., & Lucek, K. (2020). Speciation through
857 chromosomal fusion and fission in Lepidoptera. *Philosophical Transactions of the*
858 *Royal Society B: Biological Sciences*, 375(1806), 20190539.
859 <https://doi.org/10.1098/rstb.2019.0539>

860 Dierckxsens, N., Mardulyn, P., & Smits, G. (2017). NOVOPlasty: De novo assembly of
861 organelle genomes from whole genome data. *Nucleic Acids Research*, 45(4), e18.
862 <https://doi.org/10.1093/nar/gkw955>

863 Dincă, V., Lukhtanov, V. A., Talavera, G., & Vila, R. (2011). Unexpected layers of cryptic
864 diversity in wood white *Leptidea* butterflies. *Nature Communications*, 2, 324.
865 <https://doi.org/10.1038/ncomms1329>

866 Dudchenko, O., Batra, S. S., Omer, A. D., Nyquist, S. K., Hoeger, M., Durand, N. C.,
867 Shamim, M. S., Machol, I., Lander, E. S., Aiden, A. P., & Aiden, E. L. (2017). De
868 novo assembly of the *Aedes aegypti* genome using Hi-C yields chromosome-length
869 scaffolds. *Science*, 356(6333), 92–95. <https://doi.org/10.1126/science.aal3327>

870 Durand, N. C., Robinson, J. T., Shamim, M. S., Machol, I., Mesirov, J. P., Lander, E. S., &
871 Aiden, E. L. (2016). Juicebox Provides a Visualization System for Hi-C Contact Maps
872 with Unlimited Zoom. *Cell Systems*, 3(1), 99–101.
873 <https://doi.org/10.1016/j.cels.2015.07.012>

874 Durand, N. C., Shamim, M. S., Machol, I., Rao, S. S. P., Huntley, M. H., Lander, E. S., &
875 Aiden, E. L. (2016). Juicer Provides a One-Click System for Analyzing Loop-
876 Resolution Hi-C Experiments. *Cell Systems*, 3(1), 95–98.
877 <https://doi.org/10.1016/j.cels.2016.07.002>

878 Espeland, M., Breinholt, J., Willmott, K. R., Warren, A. D., Vila, R., Toussaint, E. F. A.,
879 Maunsell, S. C., Aduse-Poku, K., Talavera, G., Eastwood, R., Jarzyna, M. A.,
880 Guralnick, R., Lohman, D. J., Pierce, N. E., & Kawahara, A. Y. (2018). A
881 Comprehensive and Dated Phylogenomic Analysis of Butterflies. *Current Biology*:
882 *CB*, 28(5), 770-778.e5. <https://doi.org/10.1016/j.cub.2018.01.061>

883 Faria, R., & Navarro, A. (2010). Chromosomal speciation revisited: Rearranging theory with
884 pieces of evidence. *Trends in Ecology & Evolution*, 25(11), 660–669.
885 <https://doi.org/10.1016/j.tree.2010.07.008>

886 Faulkner, J. S. (1972). Chromosome studies on Carex section Acutae in north-west Europe.
887 *Botanical Journal of the Linnean Society*, 65(3), 271–301.
888 <https://doi.org/10.1111/j.1095-8339.1972.tb00120.x>

889 Fraïsse, C., Picard, M. A. L., & Vicoso, B. (2017). The deep conservation of the Lepidoptera
890 Z chromosome suggests a non-canonical origin of the W. *Nature Communications*,
891 8(1), 1486. <https://doi.org/10.1038/s41467-017-01663-5>

892 Hill, J., Rastas, P., Hornett, E. A., Neethiraj, R., Clark, N., Morehouse, N., Celorio-Mancera,
893 M. de la P., Cols, J. C., Dirksen, H., Meslin, C., Keehnen, N., Pruijscher, P.,
894 Sikkink, K., Vives, M., Vogel, H., Wiklund, C., Woronik, A., Boggs, C. L., Nylin, S., &
895 Wheat, C. W. (2019). Unprecedented reorganization of holocentric chromosomes
896 provides insights into the enigma of lepidopteran chromosome evolution. *Science
897 Advances*, 5(6), eaau3648. <https://doi.org/10.1126/sciadv.aau3648>

898 Höök, L., Leal, L., Talla, V., & Backström, N. (2019). Multilayered Tuning of Dosage
899 Compensation and Z-Chromosome Masculinization in the Wood White (Leptidea
900 sinapis) Butterfly. *Genome Biology and Evolution*, 11(9), 2633–2652.
901 <https://doi.org/10.1093/gbe/evz176>

902 Iannucci, A., Altmanová, M., Ciofi, C., Ferguson-Smith, M., Milan, M., Pereira, J. C., Pether,
903 J., Rehák, I., Rovatsos, M., Stanyon, R., Velenský, P., Ráb, P., Kratochvíl, L., &
904 Johnson Pokorná, M. (2019). Conserved sex chromosomes and karyotype evolution
905 in monitor lizards (Varanidae). *Heredity*, 123(2), 215–227.
906 <https://doi.org/10.1038/s41437-018-0179-6>

907 Jones, P., Binns, D., Chang, H.-Y., Fraser, M., Li, W., McAnulla, C., McWilliam, H., Maslen,
908 J., Mitchell, A., Nuka, G., Pesseat, S., Quinn, A. F., Sangrador-Vegas, A.,
909 Scheremetjew, M., Yong, S.-Y., Lopez, R., & Hunter, S. (2014). InterProScan 5:
910 Genome-scale protein function classification. *Bioinformatics*, 30(9), 1236–1240.
911 <https://doi.org/10.1093/bioinformatics/btu031>

912 Jurka, J. (1998). Repeats in genomic DNA: Mining and meaning. *Current Opinion in*
913 *Structural Biology*, 8(3), 333–337. [https://doi.org/10.1016/s0959-440x\(98\)80067-5](https://doi.org/10.1016/s0959-440x(98)80067-5)

914 Kandul, N. P., Lukhtanov, V. A., & Pierce, N. E. (2007). Karyotypic diversity and speciation in
915 *Agrodiaetus* butterflies. *Evolution; International Journal of Organic Evolution*, 61(3),
916 546–559. <https://doi.org/10.1111/j.1558-5646.2007.00046.x>

917 Kawahara, A. Y., & Breinholt, J. W. (2014). Phylogenomics provides strong evidence for
918 relationships of butterflies and moths. *Proceedings of the Royal Society B: Biological*
919 *Sciences*, 281(1788), 20140970. <https://doi.org/10.1098/rspb.2014.0970>

920 Kawakami, T., Butlin, R. K., Adams, M., Paull, David. J., & Cooper, S. J. B. (2009). Genetic
921 Analysis of a Chromosomal Hybrid Zone in the Australian Morabine Grasshoppers
922 (*vandiemenella*, *Viatica* Species Group). *Evolution*, 63(1), 139–152.
923 <https://doi.org/10.1111/j.1558-5646.2008.00526.x>

924 Kohany, O., Gentles, A. J., Hankus, L., & Jurka, J. (2006). Annotation, submission and
925 screening of repetitive elements in Repbase: RepbaseSubmitter and Censor. *BMC*
926 *Bioinformatics*, 7(1), 474. <https://doi.org/10.1186/1471-2105-7-474>

927 Korf, I. (2004). Gene finding in novel genomes. *BMC Bioinformatics*, 5(1), 59.
928 <https://doi.org/10.1186/1471-2105-5-59>

929 Krueger, F. (2019). *Babraham Bioinformatics—Trim Galore!*
930 https://www.bioinformatics.babraham.ac.uk/projects/trim_galore/

931 Krzywinski, M., Schein, J., Birol, I., Connors, J., Gascoyne, R., Horsman, D., Jones, S. J., &
932 Marra, M. A. (2009). Circos: An information aesthetic for comparative genomics.
933 *Genome Research*, 19(9), 1639–1645. <https://doi.org/10.1101/gr.092759.109>

934 Laetsch, D. R., & Blaxter, M. L. (2017). *BlobTools: Interrogation of genome assemblies*
935 (6:1287). F1000Research. <https://doi.org/10.12688/f1000research.12232.1>

936 Larson, A., Prager, E. M., & Wilson, A. C. (1984). Chromosomal evolution, speciation and
937 morphological change in vertebrates: The role of social behaviour. In M. D. Bennett,
938 A. Gropp, & U. Wolf (Eds.), *Chromosomes Today: Volume 8 Proceedings of the*
939 *Eighth International Chromosome Conference held in Lübeck, West Germany, 21–24*
940 *September 1983* (pp. 215–228). Springer Netherlands. https://doi.org/10.1007/978-94-010-9163-3_20

941

942 Lewis, J. J., Cicconardi, F., Martin, S. H., Reed, R. D., Danko, C. G., & Montgomery, S. H.
943 (2021). The Dryas iulia Genome Supports Multiple Gains of a W Chromosome from a
944 B Chromosome in Butterflies. *Genome Biology and Evolution*, 13(7), evab128.
945 <https://doi.org/10.1093/gbe/evab128>

946 Li, H. (2011). Improving SNP discovery by base alignment quality. *Bioinformatics*, 27(8),
947 1157–1158. <https://doi.org/10.1093/bioinformatics/btr076>

948 Li, H. (2013). Aligning sequence reads, clone sequences and assembly contigs with BWA-
949 MEM (arXiv:1303.3997). arXiv. <https://doi.org/10.48550/arXiv.1303.3997>

950 Li, H., Handsaker, B., Wysoker, A., Fennell, T., Ruan, J., Homer, N., Marth, G., Abecasis,
951 G., Durbin, R., & 1000 Genome Project Data Processing Subgroup. (2009). The
952 Sequence Alignment/Map format and SAMtools. *Bioinformatics (Oxford, England)*,
953 25(16), 2078–2079. <https://doi.org/10.1093/bioinformatics/btp352>

954 Lohse, K., Höök, L., Näsvall, K., & Backström, N. (2022). The genome sequence of the wood
955 white butterfly, *Leptidea sinapis* (Linnaeus, 1758). *Welcome Open Research*,
956 *Submitted*.

957 Lukhtanov, V. A., Dincă, V., Friberg, M., Šíchová, J., Olofsson, M., Vila, R., Marec, F., &
958 Wiklund, C. (2018). Versatility of multivalent orientation, inverted meiosis, and
959 rescued fitness in holocentric chromosomal hybrids. *Proceedings of the National
960 Academy of Sciences*, 115(41), E9610–E9619.
961 <https://doi.org/10.1073/pnas.1802610115>

962 Lukhtanov, V. A., Dincă, V., Friberg, M., Vila, R., & Wiklund, C. (2020). Incomplete Sterility of
963 Chromosomal Hybrids: Implications for Karyotype Evolution and Homoploid Hybrid
964 Speciation. *Frontiers in Genetics*, 11. <https://doi.org/10.3389/fgene.2020.583827>

965 Lukhtanov, V. A., Dincă, V., Talavera, G., & Vila, R. (2011). Unprecedented within-species
966 chromosome number cline in the Wood White butterfly *Leptidea sinapis* and its
967 significance for karyotype evolution and speciation. *BMC Evolutionary Biology*, 11,
968 109. <https://doi.org/10.1186/1471-2148-11-109>

969 Marçais, G., Delcher, A. L., Phillippy, A. M., Coston, R., Salzberg, S. L., & Zimin, A. (2018).
970 MUMmer4: A fast and versatile genome alignment system. *PLoS Computational
971 Biology*, 14(1), e1005944. <https://doi.org/10.1371/journal.pcbi.1005944>

972 Marks, P., Garcia, S., Barrio, A. M., Belhocine, K., Bernate, J., Bharadwaj, R., Bjornson, K.,
973 Catalanotti, C., Delaney, J., Fehr, A., Fiddes, I. T., Galvin, B., Heaton, H., Herschleb,
974 J., Hindson, C., Holt, E., Jabara, C. B., Jett, S., Keivanfar, N., ... Church, D. M.
975 (2019). Resolving the full spectrum of human genome variation using Linked-Reads.
976 *Genome Research*, 29(4), 635–645. <https://doi.org/10.1101/gr.234443.118>

977 Martin, M. (2011). Cutadapt removes adapter sequences from high-throughput sequencing
978 reads. *EMBnet.Journal*, 17(1), 10–12. <https://doi.org/10.14806/ej.17.1.200>

979 Mathers, T. C., Wouters, R. H. M., Mugford, S. T., Swarbreck, D., van Oosterhout, C., &
980 Hogenhout, S. A. (2021). Chromosome-Scale Genome Assemblies of Aphids Reveal
981 Extensively Rearranged Autosomes and Long-Term Conservation of the X
982 Chromosome. *Molecular Biology and Evolution*, 38(3), 856–875.
983 <https://doi.org/10.1093/molbev/msaa246>

984 Mayrose, I., & Lysak, M. A. (2021). The Evolution of Chromosome Numbers: Mechanistic
985 Models and Experimental Approaches. *Genome Biology and Evolution*, 13(2),
986 evaa220. <https://doi.org/10.1093/gbe/evaa220>

987 McKenna, A., Hanna, M., Banks, E., Sivachenko, A., Cibulskis, K., Kernytsky, A., Garimella,
988 K., Altshuler, D., Gabriel, S., Daly, M., & DePristo, M. A. (2010). The Genome
989 Analysis Toolkit: A MapReduce framework for analyzing next-generation DNA
990 sequencing data. *Genome Research*, 20(9), 1297–1303.
991 <https://doi.org/10.1101/gr.107524.110>

992 Melters, D. P., Paliulis, L. V., Korf, I. F., & Chan, S. W. L. (2012). Holocentric chromosomes:
993 Convergent evolution, meiotic adaptations, and genomic analysis. *Chromosome
994 Research*, 20(5), 579–593. <https://doi.org/10.1007/s10577-012-9292-1>

995 Miller, W. J., & Capy, P. (2004). Mobile genetic elements as natural tools for genome
996 evolution. *Methods in Molecular Biology (Clifton, N.J.)*, 260, 1–20.
997 <https://doi.org/10.1385/1-59259-755-6:001>

998 Mongue, A. J., Nguyen, P., Voleníková, A., & Walters, J. R. (2017). Neo-sex Chromosomes
999 in the Monarch Butterfly, *Danaus plexippus*. *G3 Genes/Genomes/Genetics*, 7(10),
1000 3281–3294. <https://doi.org/10.1534/g3.117.300187>

1001 Mongue, A. J., & Walters, J. R. (2018). The Z chromosome is enriched for sperm proteins in
1002 two divergent species of Lepidoptera. *Genome*, 61(4), 248–253.
1003 <https://doi.org/10.1139/gen-2017-0068>

1004 Nanda, I., Schlegelmilch, K., Haaf, T., Schartl, M., & Schmid, M. (2008). Synteny
1005 conservation of the Z chromosome in 14 avian species (11 families) supports a role
1006 for Z dosage in avian sex determination. *Cytogenetic and Genome Research*, 122(2),
1007 150–156. <https://doi.org/10.1159/000163092>

1008 Nguyen, P., Sýkorová, M., Šíchová, J., Kůta, V., Dalíková, M., Čapková Frydrychová, R.,
1009 Neven, L. G., Sahara, K., & Marec, F. (2013). Neo-sex chromosomes and adaptive
1010 potential in tortricid pests. *Proceedings of the National Academy of Sciences*,
1011 110(17), 6931–6936. <https://doi.org/10.1073/pnas.1220372110>

1012 Okazaki, S., Ishikawa, H., & Fujiwara, H. (1995). Structural analysis of TRAS1, a novel
1013 family of telomeric repeat-associated retrotransposons in the silkworm, *Bombyx mori*.
1014 *Molecular and Cellular Biology*, 15(8), 4545–4552.
1015 <https://doi.org/10.1128/MCB.15.8.4545>

1016 Okonechnikov, K., Conesa, A., & García-Alcalde, F. (2016). Qualimap 2: Advanced multi-
1017 sample quality control for high-throughput sequencing data. *Bioinformatics*, 32(2),
1018 292–294. <https://doi.org/10.1093/bioinformatics/btv566>

1019 Pazhenkova, E. A., & Lukhtanov, V. A. (2022). *Chromosomal conservatism vs chromosomal*
1020 *megaevolution: Enigma of karyotypic evolution in Lepidoptera* (p.
1021 2022.06.05.494852). bioRxiv. <https://doi.org/10.1101/2022.06.05.494852>

1022 Pennell, M. W., Kirkpatrick, M., Otto, S. P., Vamosi, J. C., Peichel, C. L., Valenzuela, N., &
1023 Kitano, J. (2015). Y Fuse? Sex Chromosome Fusions in Fishes and Reptiles. *PLOS*
1024 *Genetics*, 11(5), e1005237. <https://doi.org/10.1371/journal.pgen.1005237>

1025 Petitpierre, E. (1987). Why beetles have strikingly different rates of chromosomal evolution?
1026 *Elytron. Bulletin of the European Association of Coleopterology*, 1, 25–32.

1027 Poorten, T. (2018). *DotPlotly* [HTML]. <https://github.com/tpoorten/dotPlotly> (Original work
1028 published 2017)

1029 Pringle, E. G., Baxter, S. W., Webster, C. L., Papanicolaou, A., Lee, S. F., & Jiggins, C. D.
1030 (2007). Synteny and Chromosome Evolution in the Lepidoptera: Evidence From
1031 Mapping in *Heliconius melpomene*. *Genetics*, 177(1), 417–426.
1032 <https://doi.org/10.1534/genetics.107.073122>

1033 Quinlan, A. R., & Hall, I. M. (2010). BEDTools: A flexible suite of utilities for comparing
1034 genomic features. *Bioinformatics (Oxford, England)*, 26(6), 841–842.
1035 <https://doi.org/10.1093/bioinformatics/btq033>

1036 R Core Team. (2019). *R: The R Project for Statistical Computing*. <https://www.r-project.org/>

1037 Rastas, P. (2017). Lep-MAP3: Robust linkage mapping even for low-coverage whole
1038 genome sequencing data. *Bioinformatics*, 33(23), 3726–3732.
1039 <https://doi.org/10.1093/bioinformatics/btx494>

1040 Rieseberg, L. H. (2001). Chromosomal rearrangements and speciation. *Trends in Ecology &*
1041 *Evolution*, 16(7), 351–358. [https://doi.org/10.1016/s0169-5347\(01\)02187-5](https://doi.org/10.1016/s0169-5347(01)02187-5)

1042 Robinson, R. (1971). *Lepidoptera Genetics*. Pergamon Press.

1043 Román-Palacios, C., Medina, C. A., Zhan, S. H., & Barker, M. S. (2021). Animal
1044 chromosome counts reveal a similar range of chromosome numbers but with less
1045 polyploidy in animals compared to flowering plants. *Journal of Evolutionary Biology*,
1046 34(8), 1333–1339. <https://doi.org/10.1111/jeb.13884>

1047 Rovatsos, M., Vukić, J., Lymberakis, P., & Kratochvíl, L. (2015). Evolutionary stability of sex
1048 chromosomes in snakes. *Proceedings. Biological Sciences*, 282(1821), 20151992.
1049 <https://doi.org/10.1098/rspb.2015.1992>

1050 Ruckman, S. N., Jonika, M. M., Casola, C., & Blackmon, H. (2020). Chromosome number
1051 evolves at equal rates in holocentric and monocentric clades. *PLOS Genetics*,
1052 16(10), e1009076. <https://doi.org/10.1371/journal.pgen.1009076>

1053 Sahara, K., Yoshido, A., & Traut, W. (2012). Sex chromosome evolution in moths and
1054 butterflies. *Chromosome Research*, 20(1), 83–94. <https://doi.org/10.1007/s10577-011-9262-z>

1055

1056 Sambrook, J., & Russell, D. W. (2006). Purification of nucleic acids by extraction with
1057 phenol:chloroform. *CSH Protocols*, 2006(1), pdb.prot4455.
1058 <https://doi.org/10.1101/pdb.prot4455>

1059 Šíchová, J., Ohno, M., Dincă, V., Watanabe, M., Sahara, K., & Marec, F. (2016). Fissions,
1060 fusions, and translocations shaped the karyotype and multiple sex chromosome
1061 constitution of the northeast-Asian wood white butterfly, *Leptidea amurensis*.
1062 *Biological Journal of the Linnean Society*, 118(3), 457–471.
1063 <https://doi.org/10.1111/bij.12756>

1064 Šíchová, J., Voleníková, A., Dincă, V., Nguyen, P., Vila, R., Sahara, K., & Marec, F. (2015).
1065 Dynamic karyotype evolution and unique sex determination systems in *Leptidea*
1066 wood white butterflies. *BMC Evolutionary Biology*, 15, 89.
1067 <https://doi.org/10.1186/s12862-015-0375-4>

1068 Simão, F. A., Waterhouse, R. M., Ioannidis, P., Kriventseva, E. V., & Zdobnov, E. M. (2015).
1069 BUSCO: Assessing genome assembly and annotation completeness with single-
1070 copy orthologs. *Bioinformatics*, 31(19), 3210–3212.
1071 <https://doi.org/10.1093/bioinformatics/btv351>
1072 Smit, A., & Hubley, R. (2017). *RepeatModeler*.
1073 <https://www.repeatmasker.org/RepeatModeler/>
1074 Smit, A., Hubley, R., & Green, P. (2019). *RepeatMasker*. <https://www.repeatmasker.org/>
1075 Sotero-Caio, C. G., Volleth, M., Hoffmann, F. G., Scott, L., Wichman, H. A., Yang, F., &
1076 Baker, R. J. (2015). Integration of molecular cytogenetics, dated molecular
1077 phylogeny, and model-based predictions to understand the extreme chromosome
1078 reorganization in the Neotropical genus *Tonatia* (Chiroptera: Phyllostomidae). *BMC
1079 Evolutionary Biology*, 15(1), 220. <https://doi.org/10.1186/s12862-015-0494-y>
1080 Stanke, M., Diekhans, M., Baertsch, R., & Haussler, D. (2008). Using native and syntenically
1081 mapped cDNA alignments to improve de novo gene finding. *Bioinformatics*, 24(5),
1082 637–644. <https://doi.org/10.1093/bioinformatics/btn013>
1083 Suomalainen, E. (1953). The Kinetochore and the Bivalent Structure in the Lepidoptera.
1084 *Hereditas*, 39(1–2), 88–96. <https://doi.org/10.1111/j.1601-5223.1953.tb03403.x>
1085 Sylvester, T., Hjelmen, C. E., Hanrahan, S. J., Lenhart, P. A., Johnston, J. S., & Blackmon,
1086 H. (2020). Lineage-specific patterns of chromosome evolution are the rule not the
1087 exception in Polyneoptera insects. *Proceedings of the Royal Society B: Biological
1088 Sciences*, 287(1935), 20201388. <https://doi.org/10.1098/rspb.2020.1388>
1089 Takahashi, H., Okazaki, S., & Fujiwara, H. (1997). A New Family of Site-Specific
1090 Retrotransposons, SART1, Is Inserted into Telomeric Repeats of the Silkworm,
1091 *Bombyx Mori*. *Nucleic Acids Research*, 25(8), 1578–1584.
1092 <https://doi.org/10.1093/nar/25.8.1578>
1093 Talla, V., Soler, L., Kawakami, T., Dincă, V., Vila, R., Friberg, M., Wiklund, C., & Backström,
1094 N. (2019). Dissecting the Effects of Selection and Mutation on Genetic Diversity in

1095 Three Wood White (Leptidea) Butterfly Species. *Genome Biology and Evolution*,
1096 11(10), 2875–2886. <https://doi.org/10.1093/gbe/evz212>

1097 Talla, V., Suh, A., Kalsoom, F., Dinca, V., Vila, R., Friberg, M., Wiklund, C., & Backström, N.
1098 (2017). Rapid Increase in Genome Size as a Consequence of Transposable Element
1099 Hyperactivity in Wood-White (Leptidea) Butterflies. *Genome Biology and Evolution*,
1100 9(10), 2491–2505. <https://doi.org/10.1093/gbe/evx163>

1101 Tang, M., He, S., Gong, X., Lü, P., Taha, R. H., & Chen, K. (2021). High-Quality de novo
1102 Chromosome-Level Genome Assembly of a Single *Bombyx mori* With BmNPV
1103 Resistance by a Combination of PacBio Long-Read Sequencing, Illumina Short-Read
1104 Sequencing, and Hi-C Sequencing. *Frontiers in Genetics*, 12, 718266.
1105 <https://doi.org/10.3389/fgene.2021.718266>

1106 Traut, W., Sahara, K., & Marec, F. (2007). Sex Chromosomes and Sex Determination in
1107 Lepidoptera. *Sexual Development*, 1(6), 332–346. <https://doi.org/10.1159/000111765>

1108 Turner, J. R. G., & Sheppard, P. M. (1975). Absence of crossing-over in female butterflies
1109 (*Heliconius*). *Heredity*, 34(2), 265–269. <https://doi.org/10.1038/hdy.1975.29>

1110 Vicoso, B. (2019). Molecular and evolutionary dynamics of animal sex-chromosome
1111 turnover. *Nature Ecology & Evolution*, 3(12), 1632–1641.
1112 <https://doi.org/10.1038/s41559-019-1050-8>

1113 Wang, Y., Tang, H., Debarry, J. D., Tan, X., Li, J., Wang, X., Lee, T., Jin, H., Marler, B., Guo,
1114 H., Kissinger, J. C., & Paterson, A. H. (2012). MCScanX: A toolkit for detection and
1115 evolutionary analysis of gene synteny and collinearity. *Nucleic Acids Research*,
1116 40(7), e49. <https://doi.org/10.1093/nar/gkr1293>

1117 Weisenfeld, N. I., Kumar, V., Shah, P., Church, D. M., & Jaffe, D. B. (2017). Direct
1118 determination of diploid genome sequences. *Genome Research*, 27(5), 757–767.
1119 <https://doi.org/10.1101/gr.214874.116>

1120 Wingett, S. W., & Andrews, S. (2018). FastQ Screen: A tool for multi-genome mapping and
1121 quality control. *F1000Research*, 7, 1338.
1122 <https://doi.org/10.12688/f1000research.15931.2>

1123 Yoshido, A., Šíchová, J., Pospíšilová, K., Nguyen, P., Voleníková, A., Šafář, J., Provazník,
1124 J., Vila, R., & Marec, F. (2020). Evolution of multiple sex-chromosomes associated
1125 with dynamic genome reshuffling in *Leptidea* wood-white butterflies. *Heredity*, 125(3),
1126 138–154. <https://doi.org/10.1038/s41437-020-0325-9>
1127